HHS Public Access

Author manuscript

Anal Biochem. Author manuscript; available in PMC 2019 December 09.

Published in final edited form as:

Anal Biochem. 2001 November 01; 298(1): 1–24. doi:10.1006/abio.2001.5377.

Radiative Decay Engineering: Biophysical and Biomedical Applications

Joseph R. Lakowicz

Center for Fluorescence Spectroscopy, Department of Biochemistry and Molecular Biology, University of Maryland at Baltimore, 725 W. Lombard Street, Baltimore, Maryland 21201

Abstract

Fluorescence spectroscopy is a widely used research tool in biochemistry and molecular biology. Fluorescence has also become the dominant method enabling the revolution in medical diagnostics, DNA sequencing, and genomics. To date all the fluorescence observables, including spectral shifts, anisotropies, quantum yields, and lifetimes, have all been utilized in basic and applied uses of fluorescence. In this forward-looking article we describe a new opportunity in fluorescence, radiative decay engineering (RDE). By RDE we mean modifying the emission of fluorophores or chromophores by increasing or decreasing their radiative decay rates. In most fluorescence experiments the radiative rates are not changed because these rates depend on the extinction coefficient of the fluorophore. This intrinsic rate is not changed by quenching and is only weakly dependent on environmental effects. Spectral changes are usually caused by changes in the nonradiative rates resulting from quenching or resonance energy transfer. These processes affect the emission by providing additional routes for decay of the excited states without emission. In contrast to the relatively constant radiative rates in free solution, it is known that the radiative rates can be modified by placing the fluorophores at suitable distances from metallic surfaces and particles. This Review summarizes results from the physics literature which demonstrate the effects of metallic surfaces, colloids, or islands on increasing or decreasing emissive rates, increasing the quantum yields of low quantum yield chromophores, decreasing the lifetimes, and directing the typically isotropic emission in specific directions. These effects are not due to reflection of the emitted photons, but rather as the result of the fluorophore dipole interacting with free electrons in the metal. These interactions change the intensity and temporal and spatial distribution of the radiation. We describe the unusual effects expected from increases in the radiative rates with reference to intrinsic and extrinsic biochemical fluorophores. For instance, the decreased lifetime can result in an effective increase in photostability. Proximity to nearby metallic surfaces can also increase the local field and modify the rate of excitation. We predict that the appropriate localization of fluorophores near particles can result in usefully high emission from “nonfluorescent” molecules and million-fold increases in the number of photons observable from each fluorophore. We also describe how RDE can be applied to medical testing and biotechnology. As one example we predict that nearby metal surfaces can be used to increase the low intrinsic quantum yields of nucleic acids and make unlabeled DNA detectable using its intrinsic metal-enhanced fluorescence.

Fluorescence spectroscopy is one of the dominant tools used for biochemical research and has become the dominant method enabling the revolution in DNA sequencing and genomics. The basic principles of fluorescence are well understood, including factors which affect the

emission, such as quenching, environmental effects, resonance energy transfer (RET),[1] and rotational motions. All these effects are used to study the structure and dynamics of macromolecules and the interactions of macromolecules with each other. For example, quenching can reveal the exposure of fluorophores to the solvent or to other nearby quenching groups within the same macromolecule. RET reveals proximity between donors and acceptors located at regions of interest on the macromolecule(s), and anisotropy decays reveal the internal dynamics and segmental motions of proteins and membranes. Measurements of intensity, energy transfer, and anisotropy are also widely used in measurements of DNA hybridization, drug discovery, and fluorescence immunoassays.

In most applications of fluorescence the spectral properties of the fluorophore are altered by rate processes which modify the nonradiative decay rates of the excited state population. Both collisional quenching and energy transfer provide nonradiative pathways to the ground state. Quenching and RET have no significant effect on the rate of radiative decay, that is, the spontaneous rate at which fluorophores emit photons. The emissive rate of a fluorophore in free space is determined mostly by the excitation coefficient and absorption spectrum of the fluorophore (1). By free space we mean a homogeneous, nonconducting medium. However, an opportunity to control the radiative rates arises from the interactions of fluorophores with nearby metallic surfaces or particles. By metallic surface we mean conducting metals, not metal ions or oxides. An ability to modify the radiative decay rate can have profound implications for the use of fluorescence in basic research and technology applications. This effect is unusual and the implications of increasing the radiative rates for fluorescence have not been considered.

This Review describes the unusual spectral properties and opportunities available if one can increase the radiative decay rates. We refer to control of the radiative rates as radiative decay engineering (RDE) because an increase in the radiative decay rate is perhaps the most unusual effect of a metallic surface. However, metallic surfaces and particles can also concentrate the incident light field and alter the rate of excitation. We first describe the spectral changes expected if the radiative rate can be modified. We then briefly summarize the results from the physics literature using the most informative theoretical and experimental results on the effects of metal surfaces on fluorophores. We then describe how RDE can be applied to biochemical fluorescence and how RDE can be used in biomedical applications such as diagnostics and genomics.

The use of metal surfaces to manipulate the spectral properties of fluorophores is in its infancy. These phenomena have not been collectively explained within the framework of fluorescence spectroscopy. The viewpoint of biological fluorescence allows us to anticipate the enormous potential of RDE in biophysics, cell imaging, and diagnostics. Progress in the understanding and applications of RDE will require interdisciplinary efforts between physicists, engineers, chemists, and biologists. It will be necessary to design and construct appropriate nanoscale or mesoscale devices, and to interpret the complex spectral observations. It seems unlikely that any one individual or laboratory could accomplish all but a small fraction of the opportunities provided by RDE. For this reason we hope to stimulate further work in this field by describing our concept of radiative decay engineering

and hopefully to stimulate further work in this field. In our opinion, RDE can result in profound changes in how we think about fluorescence and its many applications.

RADIATIVE DECAY ENGINEERING

Prior to describing the unusual effects of metal surfaces on fluorescence it is valuable to describe what we mean by RDE and in particular spectral changes expected for increased radiative decay rates. Spectroscopists are accustomed to performing experiments using 5-to 10-Å-sized fluorophores in macroscopic solutions. Typically the solutions are transparent to the emitted radiation. There may be modest changes in refractive index, such as for a fluorophore in a membrane, but such changes have only a minor effect on the fluorescence spectral properties. In such nearly homogeneous solution, the fluorophores emit into free space and are observed in the far field. Local effects are not usually observed because of the small size of fluorophores relative to the experimental chamber. The spectral properties are well described by Maxwell's equations for an oscillating dipole radiating into free space. However, the interactions of electromagnetic radiation with physical objects can be considerably more complex. On a macroscopic scale the size and shape of radio antennae transmissions are designed with the goal of directing the radiation toward the receiver, and to take into account the interactions of the radiation with nearby objects such as the earth's surface.

For clarity we note that we are not considering reflection of the emitted photons from the metal surfaces. Reflection occurs after emission has occurred. We are considering the effects of the nearby surface on altering the "free space" condition, and modifying Maxwell's equation from their free space counterparts (2, 3). Like a radiating antenna, a fluorophore is an oscillating dipole, but one which oscillates at high frequency and radiates short wavelengths. Nearby metal surfaces can respond to the oscillating dipole and modify the rate of emission and the spatial distribution of the radiated energy. The electric field felt by a fluorophore is affected by interactions of the incident light with the nearby metal surface and also by interaction of the fluorophore oscillating dipole with the metal surface. Additionally, the fluorophore-oscillating dipole induces a field in the metal. These interactions can increase or decrease the field incident on the fluorophore and increase or decrease the radiative decay rate. These effects are sometimes described in terms of the photonic mode density. A large mode density provides more radiative decay pathways and larger radiative decay rates. As one may imagine the theory for such effects is complex. We will describe these effects in an intuitive manner with minimal use of theory.

Much of our knowledge and intuition about optical spectroscopy is based on measurements in fluorophores which radiate into free space. However, there are several important exceptions to the free space condition which result in dramatic spectral changes in different areas of spectroscopy. One well-known example is surface-enhanced Raman scattering (SERS) (4–9). It is known that the presence of a metal surface close to the chromophore can enhance the Raman signal by factors of 10^3 to 10^5. These enhancements are large enough to allow detection of the Raman signal of a single molecule (10) and even a single DNA base (11). The presence of a nearby metal semitransparent film can result in quenching of fluorescence. Another example is in microscopy and total internal reflection fluorescence

(TIRF). The emission of fluorophores within 50 Å of a thin metal surface is almost completely quenched. This effect has been used in fluorescence microscopy with evanescent wave excitation (12). In optical microscopy with TIRF the metal film quenches the emission from the membranous cellular regions near the quartz–water interface and allows selective observation of the emission from the cytoplasmic regions more distant from the liquid–water interface.

In addition to quenching metal surfaces or particles can cause increases in fluorescence. Depending upon the distance and geometry, metal surfaces or particles can result in quenching of fluorescence or enhancement of fluorescence by factors of up to 1000 (13–15). The effects of metallic surfaces on fluorophores are due to at least three mechanisms. One is energy transfer quenching to these metals with a d^3 dependence (14). The quenching can be understood by damping of the dipole oscillators by the nearby metal. A second mechanism is an increase in intensity due to the metal amplifying the incident field, which has been seen for metal colloids (15–17). The enhancement can be understood as due to the metal particles on concentrating the local excitation intensity. These effects of quenching and enhancing the local fields are important. However, another more important effect of metal surfaces and particles is possible.

In our opinion a remarkable opportunity for advancing fluorescence technology is available from a less known fluorophore–metal interaction. This effect is that the nearby metal *can increase the intrinsic radiative decay rate of the fluorophore.* This is a highly unusual effect. In fluorescence spectroscopy we usually have no significant control over the radiative rate (Γ). The spectral observables of quantum yields and lifetimes are governed by the magnitudes of the radiative rate Γ and the sum of the nonradiative decay rates (k_{nr}). To understand the value of controlling the radiative decay rate (Γ) it is informative to consider how this rate affects the quantum yield Q_0 and lifetime τ_0 of a fluorophore in the absence of a metal surface. Consider the Jablonski diagram in Fig. 1 (top). The quantum yield of the fluorophore in the absence of other quenching interactions is given by

$$Q_0 = \Gamma/\left(\Gamma + k_{nr}\right). \quad [1]$$

The natural lifetime of a fluorophore (τ_N) is the inverse of the radiative decay rate ($\tau_N = \Gamma^{-1}$) or the lifetime which would be observed if their quantum yield were unity or equivalently if $k_{nr} = 0$. The quantum yield is the fraction of the excited fluorophores which decay by emission (Γ) relative to the total decay ($\Gamma + k_{nr}$), and thus by the ratio in Eq. [1]. Fluorophores with high radiative rates have high quantum yields and short lifetimes. The radiative rate is determined by the oscillator strength (extinction coefficient) of the electronic transition (1). The extinction coefficients of chromophores are only slightly dependent on their environment. The radiative decay rate is essentially constant for any given fluorophore. Hence, the quantum yield can only be increased by decreasing the nonradiative rate k_{nr}, which usually occurs at lower temperatures. The lifetime of a fluorophore is determined by the sum of the rates which depopulate the excited state. In the absence of other quenching interactions the lifetime is given by

$$\tau_0 = \left(\Gamma + k_{nr}\right)^{-1}. \quad [2]$$

The lifetime of a fluorophore can be increased or decreased by changing the value of k_{nr}. Almost invariably, the lifetimes and quantum yields increase or decrease together.

Most fluorescence experiments involve changing the rates of nonradiative decay. For instance, collisional quenching with a biomolecular rate constant k_q decreases the quantum yield and lifetime according to

$$Q = \Gamma/\left(\Gamma + k_{nr} + k_q[Qu]\right), \quad [3]$$

where $[Qu]$ is the quencher concentration. The lifetime of the quenched fluorophore is decreased by the additional nonradiative path to the ground state with a rate $k_q\,[Qu]$

$$\tau = \left(\Gamma + k_{nr} + k_q[Qu]\right)^{-1}. \quad [4]$$

Similarly, resonance energy transfer (RET) results in an additional rate process which depopulates the excited state

$$k_T = \frac{1}{\tau_0}\left(\frac{R_0}{r}\right)^6. \quad [5]$$

The decay time in the presence of energy transfer is given by

$$\tau = \left(\Gamma + k_{nr} + k_T\right)^{-1} \quad [6]$$

Both quenching and RET decrease the quantum yield and lifetime of the fluorophore. The radiative rate Γ is not changed by these processes.

The absolute and relative brightness of a fluorophore are dependent on the values of the radiative and nonradiative decay rates. For instance, the radiative decay rates of the nucleic acid bases are comparable to those of typical fluorescent probes. However, the emission is very weak ($Q_0 < 10^{-4}$) and the lifetimes very short (≈10 ps) because of the high rates of nonradiative decay ($\approx 10^{11}\ s^{-1}$) (Eq. [1]) (18, 19). Similarly, the quantum yields for phosphorescence are usually very low because the radiative decay rates are slow compared to typical nonradiative rates and quenching processes (20). For example, phosphorescence of proteins is usually not observable without rigorous exclusion of oxygen (21, 22). In general there is no way to control the lifetime or quantum yield of a fluorophore other than by altering the values of k_{nr}, $k_q[Q]$, or k_T.

The concept of modifying the radiative decay rate is unfamiliar to fluorescence spectroscopy. It is informative to consider the novel spectral effects expected by increasing the radiative rate. Assume the presence of a nearby metal (m) surface increases the radiative

rate by addition of a new rate Γ_m (Fig. 1, bottom). For the present discussion we will not consider the quenching effects of the metal (k_m). In this case the quantum yield and lifetime of the fluorophore near the metal surface are given by

$$Q_m = \frac{\Gamma + \Gamma_m}{\Gamma + \Gamma_m + k_{nr}} \quad [7]$$

$$\tau_m = \left(\Gamma + \Gamma_m + k_{nr}\right). \quad [8]$$

These equations result in unusual predictions for a fluorophore near a metal surface. As the value of Γ_m increases, the quantum yield increases while the lifetime decreases. To illustrate this point we calculated the lifetime and quantum yield for fluorophores with an assumed natural lifetime τ_N = 10 ns, $\Gamma = 10^8\ s^{-1}$ and various values for the nonradiative decay rates and quantum yields. The values of k_{nr} varied from 0 to $9.9 \times 10^7\ s^{-1}$, resulting in quantum yields from 1.0 to 0.01. Suppose the metal results in increasing values of Γ_m. Since Γ_m is a rate process returning the fluorophore to the ground state, the lifetime decreases as Γ_m becomes comparable and larger than Γ (Fig. 2, top). This is a typical result, similar to that which occurs for increasing amounts of collisional quenching (Fig. 3, top). However, an unusual effect is expected for the quantum yield. As Γ_m increases, the quantum yield increases (Fig. 2, bottom). The most dramatic relative changes are found for fluorophores with the lowest quantum yields. If Q = 1.0, then changing Γ_m has no effect. If Q is low, such as 0.1 in Fig. 2, the metal-induced rate Γ_m increases the quantum yield. At sufficiently high values of Γ_m, the quantum yields of all fluorophores approach 1.0. Examination of Fig. 2 reveals that larger values of Γ_m/Γ are required to change the lifetime or quantum yield of low quantum yield fluorophores. This effect occurs because, for the same unquenched lifetime τ_0, lower quantum yields imply larger values of k_{nr}. Larger values of Γ_m are required to compete with the larger values of k_{nr}.

It is informative to compare the effects of increasing values of Γ_m with increasing amounts of quenching. Figure 3 shows this comparison in terms of the Stern–Volmer plots. The effects of the rate Γ_m are dramatically different from the effects of the rate-collisional quenching k_q [*Qu*]. In the case of collisional quenching both the lifetimes and quantum yields decrease (Fig. 3). The effects of metallic colloids which increase Γ_m are dramatically different. In this case the lifetimes decrease but the quantum yields increase. We note that the colloid “Stern–Volmer plots” are not necessarily linear and are only meant to illustrate the different effects of colloids and quenchers.

The increases in quantum yields which can occur near metal surfaces are different from the typical increase in quantum yield which occurs when a solvent-sensitive fluorophore like ANS is dissolved in a low polarity solvent or binds to a protein (23, 24). In these cases the quantum yield increases because of a decrease in the nonradiative decay rate k_{nr} (Eq. [1]).

REVIEW OF METALLIC SURFACE EFFECTS ON FLUORESCENCE

A moderately extensive physics literature on the effects of metals on fluorophores exists. In this section we provide a selected summary of those results which we feel demonstrate the types of effects which have been observed. Many of these studies use metal islands, metal colloids, metal surfaces, or mirrors. More dramatic effects have been found for islands and colloids rather than for continuous metallic surfaces.

The possibility of altering the radiative decay rates was demonstrated by measurements of the decay times of europium (Eu^{3+}) complex positioned at various distances from a planar silver mirror (25–28). In a mirror the metal layer is thicker than the optical wavelength. The lifetimes oscillate with distance but remain a single exponential at each distance (Fig. 4). This effect can be explained by changes in the phase of the reflected field with distance and the effects of this reflected field on the fluorophore. A decrease in lifetime is found when the reflected field is in-phase with the fluorophore's oscillating dipole. An increase in the lifetime is found if the reflected field is out-of-phase with the oscillating dipole. As the distance increases, the amplitude of the oscillations decreases. The effects of a plane mirror occur over distances comparable to the excitation and emission wavelengths. At short distances below 20 nm the emission is quenched. This effect is due to coupling of the dipole to oscillating surface changes on the surface of the metal, which are called surface plasmons resonances (SPR). Even more remarkable is the behavior of excited states between two perfect planar mirrors. If the distance between the mirrors is less than $\lambda/2$, then the excited state does not decay (29); that is, the lifetime becomes infinite. Since there are no perfect mirrors, and since it will be necessary to transmit light into and out of the space between the mirrors, the experimental lifetimes will be finite. However, we expect significant increases in the decay times with this moderately simple geometric configuration.

The effects of metallic surfaces on optical spectra are strongly dependent on the nature of the metal surface and/or metal particles. In most cases more dramatic effects are observed for metal colloids than planar mirrored surfaces. For example, Raman signals are remarkably enhanced by metal colloids or islands (30, 31), which has resulted in the field of SERS. Silver island films are made by depositing silver on a glass substrate. Under suitable conditions the glass becomes covered with approximate circular islands about 200 Å in diameter. About 40% of the surface is covered by the silver. If the silver were uniformly distributed, the mass thickness is typically near 40 Å. Silver island films are distinct from semitransparent metallic surfaces. These continuous surfaces are obtained at higher mass thicknesses, but for thickness less than optical wavelengths.

One of the most dramatic effects of silver islands on fluorescence is shown in Fig. 5. Silver islands were coated with a thin film of Eu $(ETA)_3$, where ETA is a ligand which chelates europium. This chelate displayed a quantum yield near 0.4. The sample contained an inert coating between the islands so Eu^{3+} chelates positioned between the islands were not emissive. When the Eu $(ETA)_3$ chelate was deposited on the silica substrate, without the silver islands, it displayed a single exponential decay time of 280 μs and a quantum yield near 0.4. However, when deposited on silver island films, the intensity increases about 5-fold and the lifetime decreases by about 100-fold to near 2 μs (Fig. 5). Also, the decay is no

longer a single exponential on the silver island films (32). The silver islands had the remarkable effect of increasing the intensity 5-fold while decreasing the lifetime 100-fold. Such an effect can only be explained by a increase in the radiative rate.

The fivefold increase in the quantum yield of Eu $(ETA)_3$ results in an apparent quantum yield of 2.0, which is obviously impossible. This high quantum yield is probably due to an increase in the local excitation field near the metal particle. For this reason, it is important to recognize the intensities measured on surfaces represent "apparent" quantum yields which can include an unknown factor due to incident field enhancement. This increase in the local intensity of the incident light cannot explain the decreased lifetime because an unperturbed Eu^{3+} chelate, excited by an enhanced field, would still decay with a 280-μs lifetime. According to the authors (32) the decreased lifetime is due to electromagnetic coupling between the Eu^{3+} and the silver islands.

Another example of the effects of metal islands on lifetimes is shown in Fig. 6 (33, 34). Rhodamine 6G and erythrosin were dip-coated onto silver island films with a 40-Å mass thickness. The lifetimes of both fluorophores were dramatically decreased by the islands, as can be seen by comparing the top and middle rows of Fig. 6. The effects of the islands depended on the surface density of the fluorophores. There were only moderate changes in the intensity induced by the islands. RG6 was quenched about 10-fold by the islands. If a fluorophore already has a quantum yield near unity, a metal surface cannot make the quantum yield exceed unity (Fig. 2). In such cases the dominant effect is quenching by the metal surface. In contrast, the erythrosin emission was slightly increased. This enhancement is the result of an increase in the radiative decay rate of erythrosin which increases the quantum yield and decreases the lifetime (middle right). These results are those expected for an increase in the radiative rate of high and low quantum yield fluorophores. The lower panels in Fig. 2 show the concentration quenching of R6G and erythrosin in the absence and presence of silver islands. It is important to note that the emission of both fluorophores is less prone to concentration quenching in the presence of the islands. This result is consistent with an increased radiative rate being competitive with intermolecular quenching. This result suggests that proximity to metal surfaces can be used to overcome quenching effects on fluorophores. It is important to recognize that this reversal of quenching is a through-space phenomenon and would not require any chemical modifications of the sample.

THEORY FOR FLUOROPHORE–METAL INTERACTIONS

Prior to describing the origin of these effects of metals, it is useful to review the optical properties of metal colloids and islands. Metal colloids have been used for centuries to make some colored glasses (35). The origin of the color as due to metallic colloids was first recognized by Faraday in 1857 (36). Typical absorption spectra of gold and silver colloids are shown in Figs. 7–9. The long wavelength absorption is called the surface plasmon absorption, which is due to electron oscillations on the metal surface. These spectra can be calculated for the small particle limit ($r \ll \lambda$) from the complex dielectric constant of the metal (37, 38). Larger particles display longer wavelength absorption (Fig. 7). The absorption spectra are also dependent on the shape of the particles, with prolate spheroids displaying longer absorption wavelengths (Figs. 8 and 9). Most studies of surface effects on

fluorescence have been performed using silver particles (Fig. 9) to avoid the longer wavelength absorption of gold.

There are several interactions between fluorophores and metallic surfaces (39–44). These effects are shown schematically in Fig. 10, and include quenching, enhancement of the strength of the incident light field, and an increase in the radiative decay rate of the fluorophore. Quenching occurs by Forster transfer to the surface plasmon absorption of the metal. This effect decreases with the cube of the distance (d) between the metal surface and the fluorophore (d^{-3}) (14). The quenching interaction is also described as an ohmic interaction which dissipates the energy. In addition to quenching there are two effects which determine the apparent quantum yield Y

$$Y = \left|L(\omega_{ex})\right|^2 Z(\omega_{em}). \quad [9]$$

The first term describes the local intensity. The local field is proportional to the incident field (E_0) which can be concentrated in regions near the metal particles. The term “apparent quantum yield” refers to the intensity of the samples, relative to the control sample, measured with the same intensity of the incident light. Because of this change in the incident field strength due to the metal particles, it is necessary to distinguish between the apparent (Y) and real quantum yield (Q). This distinction of the apparent field (Y) from the true quantum yield (Q) is not needed in the absence of metals because the field felt by the fluorophore is always the same for the sample and the reference. However, the metal particles concentrate the local fields. This effect has been modeled for ellipsoidal particles and the maximum enhancement in the magnitude of the local field is about 140 (41). The first term in Eq. [9] is proportional to the product of the quantum yield without metal and the amplification of the incident field. Since the light intensity is proportional to the square of the field, metal particles can result in greatly enhanced local excitation intensities.

The second term $Z(\omega_{em})$ describes the partition of energy into the radiative and nonradiative decay pathways, as modified by the metal particles. In the absence of metal this quantum yield is given by Eq. [1]. The quantum yield in the presence of the metal is given by Eq. [7]. The presence of a metal surface results in an *increase in the radiative decay rate.* Hence, the quantum yield increases. At present, the precise form of Eq. [7] is not clear. It is clear that the metal results in an increased radiative rate. However, we are not certain if the rate is additive (Eq. [7]), or if the metal-induced radiation is proportional to the intrinsic radiative rate. In this case $\Gamma_m = \gamma\Gamma$, so the equation becomes

$$Q_m = \frac{\Gamma(1+\gamma)}{\Gamma(1+\gamma)+k_{nr}}, \quad [10]$$

where $\gamma\Gamma$ is a metal-induced radiative decay rate proportional to the intrinsic radiative rate Γ. In either event the enhanced field and increased radiative rates occur at longer distances from the metal than quenching. Hence, there exists a region 50–200 Å from the metal surfaces were the emission is enhanced (Fig. 10).

It is interesting to consider how a metal surface affects fluorophores with high and low intrinsic quantum yields (Q_0). There are two limiting cases. If the dye has a high quantum yield ($Q_0 \rightarrow 1$), then the additional radiative decay rate cannot substantially increase the quantum yield. In this case energy transfer quenching to the metal will dominate and $Z(\omega_{em})$ will be less than one. The more interesting case is for low quantum yield chromophores. We use the term chromophores because the molecule can be weakly or nonfluorescent. In this case $Z(\omega_{em})$ can be as large as $1/Q_0$ (44). For this reason it is of interest to study fluorophore–metal interactions with low quantum yield fluorophores. While the actual mechanism is complex, one can imagine that the particles serve as an antenna, which, in combination with the chromophore, radiate faster than k_{nr}. This suggests that the emission from weakly fluorescent substances can be increased if they are positioned at an appropriate distance from a metal surface or colloid.

The value of chromophore–metal interactions in optical spectroscopy was demonstrated by SERS, in which the Raman lines are dramatically increased by the metal surface. The value of this enhancement is seen from recent reports of DNA detection using SERS, without the resonance effect (44–47). The enhancement is so significant that single fluorophores and single nucleotides have been detected by SERS (10, 11). Additionally, the enhancement may be due to a small fraction of the particles which display enhancements of up to 10^{15} (48, 49). SERS requires molecular contact between the surface and the molecule. It seems probable that such “hot” particles will also be found for surface-enhanced fluorescence. Furthermore, it seems probable that metal-enhanced fluorescence (MEF) will develop into a field analogous to SERS. We note that the term “surface-enhanced fluorescence” (SEF) usually refers to the incident field concentration effect, and not to modification of the radiative decay rates of fluorophores.

Theory for Metallic Particles–Fluorophore Interactions

Several groups have considered the effects of metallic spheroids on the spectral properties of nearby fluorophores (39–43). A typical model is shown in Fig. 11, for a prolate spheroid with an aspect ratio of a/b. The particle is assumed to be a metallic ellipsoid with a fluorophore positioned near the particle. The fluorophore is located outside the particle at a distance r from the center of the spheroid and a distance d from the surface. The fluorophore is located on the major axis and can be oriented parallel or perpendicular to the metallic surface.

The presence of a metallic particle can have dramatic effects on the radiative decay rate of a nearby fluorophore. Figure 12 shows the radiative rates expected for a fluorophore at various distances from the surface of a silver particle and for different orientations of the fluorophore transition moment. The most remarkable effect is for a fluorophore perpendicular to the surface of a spheroid with a/b 5 1.75. In this case the radiative rate can be enhanced by a factor of 1000-fold or greater. The effect is much smaller for a sphere (a/b = 1.0), and much smaller for a more elongated spheroid (a/b = 3.0) when the optical transition is not in resonance with the particle. In this case the radiative decay rate can be decreased by over 100-fold. If the fluorophore displays a high quantum yield or a small value of k_{nr}, this effect could result in 100-fold longer lifetimes. The magnitude of these

effects depends on the location of the fluorophore around the particle and the orientation of its dipole moment relative to the metallic surface. The dominant effect of the perpendicular orientation is thought to be due to an enhancement of the local field along the long axis along the particle.

The transition dipole–surface orientation can result in unusual effects. This is illustrated in Fig. 13, which shows the expected decay rates of a fluorophore near a solid silver surface (27). The decay depends on orientation relative to the surface. In the parallel orientation the dipole in the metal cancels the dipole in the fluorophore, which slows the decay. In the perpendicular orientation the fluorophore's dipole and the dipole in the metal are synergistic and increase the decay rate. This effect of orientation results in an unusual possibility. In almost all known cases the anisotropy decay of a fluorophore represents motions of the fluorophore and is independent of the intensity decay. For a fluorophore near a plane metal surface (Fig. 13) or a metal particle (Fig. 12), the intensity decay will be coupled to the anisotropy decay. For instance, a fluorophore oriented mostly perpendicular to the surface of a particle will decay 1000-fold faster if it can rotate rather than remain stationary.

Spatial Distribution of Emission Near Metal Surfaces

In a typical cuvette experiment the fluorophores radiate into free space. The emission from a randomly oriented population is isotropic in all directions. Even for oriented fluorophores, or for an isotropic solution excited with polarized light, the emission is nearly isotropic. As a result the sensitivity of fluorescence detection is limited by the small solid angle of light collection possible with detectors of practical size. Radiative decay engineering offers the possibility of directing the emission in specific directions, which may be toward the detector. Suppose the metallic surface has a periodic structure with a distance of 300 nm between peaks (Fig. 14). The surface is completely covered with silver; that is, there are no islands. The fluorophore was positioned above this surface with an inert spacer (50). For such a sample the intensity varies with the distance of the fluorophore above the sample (Fig. 15). Hence a fluorophore can be made fluorescent or nonfluorescent depending upon its distance from the periodic surface. It is also known that the lifetime of a fluorophore varies with distance above a periodic surface (51). Remarkably, the radiation was directed into small angular distributions, in one case with over 90% of the radiation found at two angles ±15° from the normal (Fig. 16). This effect is not due to reflection of the emitted photons, but rather to the interactions of the oscillation dipole and the oscillations electron in the metal, and their directed radiation into the space over the metal.

There is a second method for obtaining directional emission. This occurs when fluorophores are deposited directly, with no inert spacer, onto silver grating. In this case energy from the fluorophores is transferred into the metal and radiated by surface plasmon polaritrons (28, 52, 53). This remarkable result suggests the design of high-sensitivity nanoscale sample chambers which direct the emission into the detector.

To summarize this section, nearby metal surfaces can increase radiative decay rates, increase quantum yields, decrease lifetimes, and concentrate the emission into small angular distributions. The successful use of these effects can have profound implications resulting in a wide variety of novel fluorescence methods.

Comparison of Surface-Enhanced Fluorescence and Surface-Enhanced Raman Scattering

While SERS also depends on metal particles or a rough metal surface, it seems that there are different phenomena, at least in part. Surface-enhanced fluorescence and SERS show different dependencies on the distance to the surface. The enhancement of Raman scatter and fluorescence by metal colloids is illustrated in Fig. 17 (15). Silver colloids were prepared in suspension by known procedures. The particles were reacted with a glass surface which had been derivativized to contain sulfhydryl groups. This colloidal metal film was then covered with one or more layers of octadecanoic acid (ODA) as a Langmuir–Blodgett film. Each layer of ODA was thought to be 25 Å thick. A fluorescein-labeled lipid Fl-DPPE was positioned in the layer immediately adjacent to a silver-colloidal film line (line 1) and in layers more distant from the metal (lines 2–4). In the absence of metal on the bare glass slide there is little detectable emission (Fig. 17, line 5). When Fl-DPPE is immediately adjacent to the metal, the emission is enhanced, as are the Raman peaks (line 1). When Fl-DPPE is present in the more distant layers, the emission is still enhanced, but the shorter range SERS effect is no longer present. It appears that SERS requires molecular contact of the fluorophore with the metal particles. The fluorescence enhancement occurs at larger distances from the metal, up to 100 Å (curves 2 to 5). The lifetimes were not measured, so it is not known what proportion of the enhancement is due to the factors $L(\omega_{ex})$ and $Z(\omega_{em})$ in Eq. [9]. That is, the enhanced emission from Fl-DPPE could have been due to either an enhanced electric field due to the metal particles, increased radiative decay rates, or both. Since fluorescein has a moderately high quantum yield it is likely that the increased intensity was due to the increased local incident field.

Another possibility of RDE is to obtain usefully high emission from essentially nonfluorescent molecules. In a nonfluorescent molecule the nonradiative decay rates are typically much larger than the radiative rate, that is $k_{nr} \gg \Gamma$. To obtain a usefully high quantum yield the total radiative rate $\Gamma + \Gamma_m$ needs to become comparable to k_{nr}. This possibility is shown in Fig. 18 (54). Basic Fuchsin is a dye with a low quantum yield near 0.02. The probe was maintained at various distances from the silver island film by layers of SiOx. The apparent quantum yield of basic Fuchsin increased by a factor of 200 when positioned about 40 Å over film of silver island (Fig. 18). The interaction between basic Fuchsin and the metal surface appeared to be completely optical, with no known chemical interactions. The control measurements demonstrated that the effect was not due to a rigid environment for the probe. This result suggests that the quantum yield of any chromophore can be increased by placement at an appropriate distance over silver particles. Figure 18 (left) shows the distance dependence of Raman scattering for the same chromophore. The Raman scattering decreases more rapidly than the surface enhanced fluorescence.

BIOPHYSICAL APPLICATIONS OF RDE

In the preceding sections we summarized the effects of metal surfaces and particles on fluorophores. These effects are highly dependent upon distance and the nature of the metal surface. At short fluorophore–metal distances the fluorophores are quenched. At appropriate distances near 50–200 Å the radiative rates are increased. In addition to increased radiative rates, the fluorophores can also be exposed to higher local fields due to interactions of the

metal or metal particles with the incident light. Finally, these effects are expected to depend on the orientation of the oscillator dipole relative to the metal surfaces. These effects can be used in the biochemical and medical applications of fluorescence. However, the successful application radiative decay engineering will require considerable efforts in mesoscale and nanoscale fabrication, surface coating, and coupling of fluorophores and macromolecules to the surfaces. Given the complexity of these efforts, and the need for interdisciplinary collaborations, we feel it is valuable to speculate about the potential applications of RDE.

Effects of Metal Particles on Fluorophore Photostability and Detectability

In single molecule detection and in fluorescence microscopy the signal level is limited by photodecomposition of the fluorophores (55–57). Typical fluorophores can undergo a finite number of exciting emission cycles prior to photobleaching or photochemical destruction. For photostable molecules like tetramethyl–rhodamine, photodecomposition occurs after about 10^5 cycles. Less stable fluorophores will degrade after fewer cycles. Even sensitive detection systems have an overall detection efficiency near 1%. Hence, one can at most observe 10^3 from a fluorophore, and typically less (56). It would be valuable to know if fluorophore–metallic particles interactions can increase the detectability of single molecules. There are three effects to consider: quenching at short distances, an increase in the excitation field, and an increase in the radiative decay rate. These effects are shown top to bottom in Fig. 19.

First we consider the effects of quenching when the fluorophores are close to the surface (, 50 Å) (Fig. 19, solid line, top left). Assuming there is no change in the emission rate (Γ_m = 0), the intensity of the fluorophores will be decreased near the surface (Fig. 19, top left). However, it is known that quenching by RET results in increased photostability because the molecules spend less time in the excited state and thus have fewer opportunities for photochemical reactions (58). Increased photostability has also been observed on metal-island films (59). Since the lifetime of the fluorophores will be decreased (Fig. 19, top center), quenching by the surface is expected to result in increased stability and an increase in the number of excitation–deexcitation cycles prior to photodecomposition. While the quantum yield is reduced, the number of detected photons or detectability is expected to be about the same, as can be seen from the integrated area for continuous illumination (Fig. 19, upper right).

Now consider the effect of a metal-induced concentrations of the incident field felt by the fluorophore at the same illumination intensity (Fig. 19, middle panel). This effect will result in an increased intensity when compared to the no-metal sample, both observed with the same incident intensity. The intensity will be higher for the same incident intensity (Fig. 19, middle right). However, the excited molecules will have the same radiative decay rate Γ and Γ_m = 0. The lifetimes will remain the same. Since there is no quenching, we expect the same overall numbers of emitted photons until the fluorophore is destroyed, as seen from the integrated area with continuous illumination (middle right). One possible effect is that the sample may display ground state depletion at lower incident intensity of the excitation light (Fig. 20, bottom). However, we have not found any reports of alterations in the rates of

intersystem crossing or blinking due to metal surfaces. Such effects may occur, but to our knowledge have not been reported.

The lower panels in Fig. 19 illustrate the effect of an increased radiative rate. In contrast to the previous two effects, an increase in the radiative decay rate is expected to result in dramatic increases in the number of photons observed from each fluorophore. An increase in the radiative rate will result in an increased intensity due to the increased quantum yield (Fig. 19, bottom). The lifetime will be shortened by the metal-induced increase in the radiative rate. Since the fluorophore will spend less time in the excited state for each cycle, the extent of photobleaching is expected to decrease. The combination of increased quantum yield and decreased photobleaching should result in a substantially increased number of detected photons per fluorophore when the radiative rate is increased (lower right).

It is informative to speculate on the potential increases in intensity resulting from metal surfaces and particles. These effects are shown in a qualitative manner in Fig. 20. A metallic ellipsoid with an appropriate size and shape can result in a 140-fold amplification of the local intensity (44). Since the intensity is proportional to the squared field strength, these effects can result in a 10^4-fold or greater increase in the rate of excitation. This effect is shown as a larger intensity at a given illumination (Fig. 20, dotted line). In addition to enhanced excitation, location of the fluorophore at an appropriate distance from a metallic spheroid can result in an over 10^3-fold increase in the radiative decay rate (Fig. 12). Hence, at the same illumination intensity, one can expect a 10^7-fold increase in the intensity from appropriately localized fluorophores.

While a 10^7-fold enhancement is remarkable, it is possible that even larger enhancements can be found. The number of photons emitted by a single fluorophore is limited by its lifetime. As a rough estimate a fluorophore with a 10-ns lifetime can emit about 10^8 photons per second (55). This effect is illustrated in Fig. 20 when the emission intensity remains constant for higher illumination intensities due to ground state depletion. Suppose now that the metal surface reduces the lifetime 100-fold from 10 ns to 100 ps. In this case the illumination intensity can be increased until the emission rate of each molecule is 10^{10} photons per second. This effect can result in a further 100-fold increase in the instantaneous intensity, for an overall enhancement of 10^9. Finally, an appropriately designed metal chamber may direct the emission toward a detector, which could result in an additional factor of 10 or more. These known factors strongly suggest that the use of appropriate metal surfaces may result in increased ease of single molecule detection, or even visual detection of single fluorophores.

Effects of Metal Particles on Quenching

Collisional quenching occurs widely for biochemical fluorophores, and quenching is used to characterize biomolecules (60, 61). Quenching by exogenous quenchers like oxygen, iodide, and acrylamide is often used to measure local diffusion coefficients and the extent to which fluorophores are shielded from the solvent by the macromolecule. When collision occurs, both the quantum yield and lifetimes are reduced by the presence of an additional rate process which depopulates the excited state, with a rate $k_q[Qu]$ in Eqs. [3] and [4]. We have not found any reports on the effect of a metal surface on collisional quenching. It seems

unlikely that metal surfaces would have any effect on $k_q[Qu]$ except if the local quencher concentration is altered by the surface.

Suppose a fluorophore is present in a solution containing quenchers, and that one measures the emission intensity at various distances from the metal particles. Recall that collisional quenching is described by the Stern–Volmer equation

$$\frac{F_0}{F} = 1 + k_q \tau_0 [Qu], \quad [11]$$

where F_0 and F are the intensities in the absence and presence of quencher, respectively, k_q is the biomolecular quenching control, and τ_0 is the unquenched lifetime. This equation shows the well-known result that fluorophores with longer lifetimes are quenched more than those with shorter lifetimes. The intensity is expected to increase closer to the surface due to the increased radiative rate that emission competes more effectively with quenching. Hence, emission from the quenched fluorophores will be observable near the metal particles. If desired, one can use high quencher concentrations to minimize the emission from all regions of the sample except those adjacent to the metal. Alternatively, suppose that the solution contains a second fluorophore which is not accessible to the quencher, or one which displays a high quantum yield. In this case an increase in the radiative decay rate will not result in increased intensity from this second fluorophore. Thus the metal particles could be used to detect the quenched species by selective enhancement of its quantum yield.

Biological molecules contain a number of intrinsic fluorophores. A substantial fraction of intrinsic fluorophores are quenched. As examples, we note that flavins and FAD are fluorescent in solution, but most flavoproteins display little if any flavin emission (62–64). Tyrosine is often quenched in proteins, and frequently tryptophan residues are quenched by nearby amino acid residues such as disulfide bonds, histidine, or phenylalanine side chains (65–67). Another well-known example is DNA, nucleotides, and the individual bases. While some intrinsic emission has been reported (68, 69), the intrinsic fluorescence from the five common nucleic acid bases is very weak and has been of little practical usefulness.

We believe surface effects may result from usefully intense emission from all these intrinsic fluorophores. Flavoproteins adjacent to metal surfaces may become fluorescent as the increased radiative rates become comparable in magnitude to the quenching rates. Similarly, quenched residues in proteins or DNA may display useful emission if the radiative rates can be made comparable to the nonradiative decay rates. Since significant enhancements of fluorescent have been observed for basic fuchsin with its low quantum yield near 0.02, there is reason to expect similar results can be obtained for DNA.

It is instructive to consider an example. Suppose a protein has two tryptophan residues. Assume that the surface exposed is strongly quenched by a local quenching interaction. In the absence of metal, emission will only be observed from the higher quantum yield residue emitting at shorter wavelengths (Fig. 21). When the protein is close to a metal particle, both residues will emit faster. However, the quantum yield of the quenched residue will be increased to a greater extent (see Fig. 2). Hence, the spectral shape will change due to an

increased in intensity at shorter wavelengths from the increased quantum yield of the quenched residue.

Surface-enhanced radiative rates may also result in phosphorescence. Phosphorescence is usually not observable in room temperature solutions due to quenching by even low concentration impurities, and because the slow emission rates cannot complete with the faster nonradiative decay rates (Eq. [1]). If the surface increases the radiative rate of a triplet state molecule, then the quantum yield for phosphorescence should increase. Additionally, the decreased phosphorescent lifetime should decrease the extent of quenching by oxygen and other quenchers. Protein phosphorescence may become a common observation for proteins near surfaces, even in the presence of oxygen. Alternatively, there may be a subclass of tryptophan residues which are on the verge of displaying phosphorescence which becomes readily observable near surfaces.

Solvent Effects and Spectral Shifts

Many fluorophores display large Stokes' shifts. In general, polar fluorophores in polar fluid solvent display the largest Stokes' shifts. These spectral shifts are due to interactions of the excited state dipole moment of fluorophore with surrounding polar solvent molecules. The solvent must not be too viscous or glassy, in which case a blue-shifted emission is observed from fluorophores for which the solvent molecules have not yet reoriented. At intermediate viscosities the emission spectra depend on the lifetime.

The extent of solvent or spectral relaxation depends on both the solvent relaxation time (τ_R) and the fluorescence lifetime τ. This can be seen from the expression which relates the observed emission center-of-gravity $\bar{V}_{cg}$ with that found for the unrelaxed and fully relaxed states, v_0 and v_{∞}, respectively,

$$\bar{\nu}_{cg} = \bar{\nu}_{\infty} + (\bar{\nu}_0 - \bar{\nu}_{\infty})\frac{\tau_R}{\tau + \tau_R}. \quad [12]$$

This expression shows that when the relaxation time τ_R is short relative to the lifetime τ, the solvent-relaxed red-shifted emission is observed. A blue-shifted emission is observed if the solvent becomes more viscous, if τ_R becomes longer, or if the lifetime τ decreases. Hence, for polarity-sensitive fluorophores we expect a blue-shifted emission near the metal surface due to the shorter lifetime (Fig. 22).

The blue shift near a metal surface may be useful in studies of lipid bilayers or cell membranes. For example, solvent-sensitive fluorophores like prodan or laurdan display blue-shifted emission in solid-phase membranes and red-shifted emission above the phase transition temperatures (70, 71). It is also known that polarity-sensitive fluorophores display time-dependent spectral shifts when bound to proteins or membranes (72, 73). The time-resolved emission spectra shift to larger wavelengths at longer times following excitation. This is due to the similar time scales of emission and solvent relaxation. Suppose the proteins or membranes are labeled with a solvent-sensitive fluorophore like prodan or

acrylodan (74, 75). In this case it may be possible to selectively observe the labeled protein near the surface by observation on the short wavelength side of the emission.

Resonance Energy Transfer

At present there are only limited experimental results on the effects of metal particles on resonance energy transfer. However, interesting theoretical predictions have been reported (76, 77). In the absence of metal particles the rate of transfer k_T^0 depends on the donor (D) to acceptor (A) distance according to Eq. [5]. Suppose the donor and acceptor are located along the long axis of an ellipsoid with the dipoles also oriented along this axis. Figure 23 shows the enhancement of the rate of energy transfer due to the metal particle, that is the ratio of the rates of transfer in the presence (k_T^m) and absence (k_T^0) of the metal. Enhancement of 10^4 is possible. The enhancement depends on the transition energy being in resonance with the particle. A smaller but still significant enhancement is found for a less resonant particle (Fig. 23, lower curve) and on wavelength (Fig. 24). The enhanced rate of energy transfer persists for distances much larger than typical Forster distances (Figs. 23 and 24). While these simulations are for dipoles on the long axis and oriented along this axis, the enhancements are still large when the donors and acceptors have different orientations and locations around the particle (77).

The simulations in Figs. 23 and 24 do not consider the increased emission rates of fluorophores near surfaces. Since emission and RET are competitive processes, the RET efficiency depends on the relative values of the emission and energy transfer rates. Examination of the available simulations (76, 77) suggests that the enhancements in RET are larger than the enhancements in the emissive rates. This indicates that RET will occur over longer distances near metal particles even if the donor lifetimes are decreased by more rapid emission. It is important to know whether the metal-induced rates of transfer depend on the emissive rate of the donor. In the case of RET without metal particles the rate of transfer is proportional to the donor emissive rate. This can be seen from Eq. [5] by recalling that rate of transfer is proportional to the quantum yield (Q) [see Eq. 13.2, in Ref. (78)]. The ratio Q/τ_D^0, where τ_D^0 is the donor lifetime in the absence of acceptor, is proportional to the emissive rate of the donor. This means in the absence of metal that RET is 50% efficient when the D–A distance is R_0, irrespective of the unquenched lifetimes of the donor, whether the donor is a millisecond-decay-time lanthanide or a picosecond-decay-time fluorophore. It appears that the rate of transfer near the metal will be proportional to the emission rate of the donor in the absence of the particle (76, 77). Additional simulations and experiments are needed to clarify the effects of metal particles on the efficiency of RET.

At this time the implications of metal-enhanced RET for biochemistry are not known. One obvious possibility is detection of D–A proximity over long distances. For instance, one may be able to detect RET between proteins located on opposite sides of a membrane. Energy transfer between different proteins in a larger macromolecule complex may become significant in the presence of metal particles.

Effect of Fluorophore Orientation and/or Rotation on Intensity Decays

Time-resolved intensity decays reveal the rates and amplitudes of fluorophore motions during the excited state lifetime. In almost all known cases there is no direct linkage between the intensity and anisotropy decays of a fluorophore. These are independent processes. This interaction independence remains true even for associated anisotropy decays where each species in a mixture displays its own characteristic intensity and anisotropy decays (79, 80).

In Fig. 13 we described how fluorophore orientation relative to the metal surface affects its decay rate. This interaction results in an unusual effect in which the rotational rate of a fluorophore affects its lifetime. Consider a membrane deposited on a perfect mirror and assume the coexistence of solid-and liquid-phase lipids. If a fluorophore is oriented perpendicular to the surface in the solid phase, its lifetime will be shorter relative to a parallel fluorophore in the fluid-phase membrane. This effect would allow the phases to be distinguished by longer decay times in the fluid phase. Other effects are also possible. For instance, assume rotational diffusion allows the fluorophore to sample orientations which increase the decay rate, and that these dynamically accessible orientations are not found in the solid-phase membranes. In this case the fluid-phase regions of the bilayers will display shorter decay times. This effect may provide an alternative approach to identify lipid microdomains in membranes (81, 82). The emission also occurs in different directions for different observed polarizations (50). This suggests that one can observe different fluorophore populations based on their emission at various angles relative to the surface. This could be a new form of “dichroism” based on directed emission from different fluorophores. As another example, suppose the orientation of a fluorophore relative to a metal surface can be altered by an static electric field or a change in solution conditions. These changes in orientation would result in a change in the decay time.

Near-Field Microscopy

Metal effects on fluorescence have already been detected in scanning near-field optical microscopy (SNOM) (83–86). One example is shown in Fig. 25 (83). In this case there is no optical aperature. The sample is illuminated near the atomic force microscope (AFM) metal tip, but not through the tip. The emission from the sample is enhanced in a 70-Å region surrounding the AFM tip, which is measured by a nearby detector. The local field is increased about 10-fold by the tip, which results in a 100-fold increase in the local intensity. The effects of the metal tip on the local fluorescence lifetime of a Eu^{3+} sample have already been used for lifetime imaging (85). At present SNOM is being used for single molecule detection (87–89) and imaging is being done using RET between the sample and the tip (90–92). Consideration of the effects of metals on the emissive rate and energy transfer rates may suggest new types of measurements using SNOM.

SNOM may provide a valuable method to study fluorophore–metal interactions. This possibility is suggested by the effects of a gold SNOM tip on the emission from a Eu^{3+} sample (Fig. 26). In this case the lifetime from the Eu^{3+} layer was found to depend on the distance between the tip and the sample (86). One can readily imagine measurements of intensities and lifetimes in specific regions around metal islands, or the effects of metal islands on energy transfer.

BIOMEDICAL APPLICATIONS OF RDE

In the preceding sections we considered the molecular aspects of surface-enhanced fluorescence and how these effects could yield new information in biochemical research. We now consider how these effects can be used in the biomedical applications of fluorescence.

Assays Based on Low Quantum Yield Fluorophores

At present one usually strives to use the fluorophores with the highest quantum yields. When using metal surfaces it may becomes desirable to use fluorophores with low quantum yields. Consider the schematic immunoassay assay in Fig. 27. Assume that a capture antibody is covalently bound to the surface near the metal particles. The presence of the analyte (An) results in surface binding of a second antibody which is labeled with a nonfluorescent chromophore. Upon binding to the antigen the previously nonfluorescent species emits due to the increased radiative rate. The unbound species more distant from the metal site will not interfere because they do not fluoresce. The nonfluorescent species becomes a “molecular beacon” emitting only when close to the metal particles. In fact, two recent reports have shown the use of metal-enhanced emission from low quantum yield fluorophores in immunoassays (93, 94).

The concept of surface-enhanced fluorescence can be extended to assays which use electrical potential to gate the fluorescence on and off. For example, the fluorophore may be positioned at the end of a flexible polymer chain (Fig. 28). The entire chain and fluorophore can be negatively charged. If the voltage or the metal is positive, the fluorophore can be in the quenched zone. If the voltage is made negative, the fluorophore can be displaced into the enhancement zone. Alternatively, the fluorophore could be moved in and out of the shorter range quenching zone of the metal. In either case the emission could be gated by the voltage. This concept can be extended to provide a method to access array sensors (95, 96). This possibility is supported by a recent report which showed voltage-dependent emission from a fluorophore bound to a gated electrode (97).

Energy Transfer Immunoassays

Immunoassays have also been based on RET (98, 99). Typically donor- and acceptor-labeled antibodies bind to the antigens or analytes (An) (Fig. 29). Alternatively, the assay can be competitive in which case the endogenous analyte competes with donor (or acceptor)-labeled antigen. While RET immunoassays have been demonstrated in the laboratory, the large size of antibodies relative to the Forster distances has resulted in low transfer efficiencies. However, suppose the complexes migrate to a silver island surface due to an electrical potential or other attractive force. In this case the metal-induced increase in the transfer rate will result in transfer over larger distances and the antigen will become detectable by an increase in the transfer efficiency.

Enhanced energy transfer can be combined with directional emission to result in higher sensitivity. For example, it is known that fluorescence can be excited by the evanescent wave due to surface plasmons (100, 101). This experiment arrangement is shown in Fig. 30. Remarkably, the emission resulting from surface plasmon excitation is directed in a narrow

angular distribution. For the control surface without silver (right) the emission increases at the critical angle for the fluorescence. When excitation is at the plasmon resonance angle, the emission is sharply distributed at the plasmon angle for the emission wavelength. It seems possible to use this effect to selectively observe the desired signal while rejecting background at different wavelengths or distances from the silver surface.

Chemiluminescent and Electrochemiluminescent Assays

Chemiluminescence and electroluminescence are useful detection methods because the emission occurs without autofluorescence from the samples (102–104). Metal particles could be used to increase the sensitivity of these assays. For example, electroluminescent assays are often performed using ruthenium metal–ligand complexes, such as $[Ru(bpy)_3]^{2+}$ where bpy is 2,2'-bipyridine. The excited state is generated by electrochemical creation of an amine free radical. This species reacts with the oxidized Ru complex to yield an excited state complex. The quantum yields of $[Ru(bpy)_3]^{2+}$ and similar complexes are below 5%. The use of a silver island surface can increase the Ru complex quantum yield and improve sensitivity (Fig. 31). As shown in Fig. 16, a periodic metal surface can result in spatially directed emission. This suggests that a further increase in electroluminescence sensitivity could be obtained by use of an appropriate metal surface to direct the emission toward the detector (Fig. 31). We note that directed emission should occur whether the fluorophore is excited using light or chemical energy.

DNA Analysis

Completion of the human genome sequence is driving development of a wide variety of approaches to DNA analysis. These methods include DNA arrays or gene chips, PCR-based assays and hybridization assays (105–110). Many of these assays are based on RET. In the case of hybridization assays the length of the sequence needs to be small enough to position the donors and acceptors within the Forster distance (109, 110). This limitation may be overcome using metal surfaces. Since the transfer distance can be increased 10-fold more by a metal particle, one can imagine RET assays being performed where the donors and acceptors are 150 base pairs apart, rather than the more typical 15 base pairs. Alternatively, metal-enhanced RET may be used to probe longer range structures in DNA, RNA, or ribosomes.

One can imagine DNA hybridization reactions which are detected by surface effects on fluorescence or on RET. For example, it is known that the local field can be dramatically enhanced between two spherical colloids (111) (Fig. 32). Two metal colloids may be brought into close proximity by complementary single-stranded oligomers on each particle. The high field between the particles could enhance the emission of a high or low quantum yield dye bound to the hybridized DNA between the particles. The high field may enhance the extent of multiphoton excitation of the dye or of DNA itself. Alternatively, the rate of energy transfer of donors and acceptors may be enhanced between the particles.

All presently used DNA assays rely on extrinsic probes which are used to impart useful fluorescence to intrinsically nonfluorescent DNA. Radiative decay engineering can revolutionize DNA technology. Suppose DNA is adjacent to a metal surface and the

radiative decay rate is increased, or between two particles as shown in Fig. 32. Then one may be able to use the enhanced intrinsic emission of DNA, rather than labeling the DNA (Fig. 33). The deep UV absorption of DNA will not be a problem because compact 263-nm lasers are now available. Alternatively, the metal particles may facilitate two-photon or multiphoton excitation due to enhanced local fields, allowing excitation of intrinsic DNA fluorescence using visible or NIR lasers. The intrinsic emission of DNA may be different for single-and double-stranded DNA, facilitating detection of hybridization. If needed, the DNA may be electrophoresed to the metal for the analysis.

DNA Sequencing

While the human genome and other organisms have been sequenced (112, 113) there is still a need for faster, cheaper, and more sensitive DNA sequences. Some groups are attempting to sequence a single DNA strand using a single strand of DNA (114, 115). The basic idea is to allow an exonuclease to sequentially cleave single nucleotides from the strand, label the nucleotide with a fluorophore, and detect and identify the labeled nucleotide. This goal is more difficult than single molecule detection because every nucleotide must be detected and identified, not the simpler task of finding one fluorophore among many. Also, the labeling of nucleotides is likely to result in a larger number of fluorophores which have not reacted.

The use of RDE could allow base detection and identification without labeling. Suppose the released nucleotides pass through a specially designed flow chamber (Fig. 34). The size and shape of the chamber could be such that the bases displayed intrinsic emission. Also, the surface would be shaped and periodic in a manner which directs the emission toward a detector. The design would be such that the directed emission occurs wherever the unlabeled nucleotides flow through the laser beam. SERS of DNA bases has been observed using silver and gold colloids (116), which suggests to us that surface-enhanced fluorescence will also be observed for DNA and its bases. Additionally, it has now become possible to create silver particles on surfaces with broadly tunable SPR spectra using nanolithography (117), and a variety of methods are appearing for self-assembly of metallic nanoparticles (118–120). If successful, such an apparatus would allow DNA sequencing using intrinsic nucleotide fluorescence.

CONCLUSION

In the preceding sections we have described the remarkable opportunities available by combining fluorescence and metal particles. Many challenges must be met to make practical use of these known optical phenomena. The effective use of these interactions can result in new types of fluorescence experiments and novel approaches to medical diagnostics.

ACKNOWLEDGMENT

Work was supported by the NIH, National Center for Research Resources, RR-01889.

Abbreviations used:

1

AFM	atomic force microscope
MEF	metal-enhanced fluorescence
RDE	radiative decay engineering
RET	resonance energy transfer
SEF	surface-enhanced fluorescence
SERS	surface-enhanced Raman spectroscopy
SNOM	scanning near-field microscopy
SPR	surface plasmon resonance
TIRF	total internal reflection fluorescence

REFERENCES

1. Strickler SJ, and Berg RA (1962) Relationship between absorption intensity and fluorescence lifetimes of molecules. J. Chem. Phys 37, 814–822.
2. Ford GW, and Weber WH (1984) Electromagnetic interactions of molecules with metal surfaces. Phys. Rep 113, 195–287.
3. Chance RR, Prock A, and Silbey R. (1978) Molecular fluorescence and energy transfer near interfaces. Adv. Chem. Phys 37, 1–65.
4. Fleischmann M, Hendra PJ, and McQuillan AJ (1974) Raman spectra of pyridine adsorbed at a silver electrode. Chem. Phys. Letts 26(2): 163–166.
5. Jeanmaire DL, and Van Duyne RP (1977) Surface Raman spectroelectrochemistry. Part 1. Heterocyclic, aromatic, and aliphatic amines adsorbed on the anodized silver electrode, J. Electroanal. Chem 84, 1–20.
6. Pettinger B, and Gerolymatou A. (1984) Dyes adsorbed at Ag-colloids: Substitution of fluorescence by similarly efficient surface fluorescence and surface Raman scattering. Ber. Bungens. Phys. Chem 88, 359–363.
7. Kneipp K, Kneipp H, Itzkan I, Dasari RR, and Feld MS(1999) Surface-enhanced Raman scattering: A new tool for biochemistry spectroscopy. Curr. Sci 77(7), 915–924.
8. Vo-Dinh T, Stokes DL, Griffin GD, Volkan M, Kim UJ, and Simon MI (1999) Surface-enhanced Raman scattering (SERS) method and instrumentation for genomics and biomedical analysis. J. Raman Spectrosc 30, 785–793.
9. Vo-Dinh T. (1998) Surface-enhanced Raman spectroscopy using metallic nanostructures. Trends Anal. Chem 17(8–9), 557–582.
10. Nie S, and Emory SR (1997) Probing single molecules and single nanoparticles by surface-enhanced Raman scattering. Science 275, 1102–1106. [PubMed: 9027306]
11. Kneipp K, Kneipp H, Bhaskaran Kartha V, Manoharan R, Deinum G, Itzkan I, Dasari RR, and Feld MS (1998) Detection and identification of a single DNA base molecule using surface-enhanced Raman scattering (SERS). Phys. Rev. E 57(6), R6281–R6284.
12. Axelrod D, Hellen EH, and Fulbright RM (1992) Total internal reflection fluorescence In Topics in Fluorescence Spectroscopy: Biochemical Applications (Lakowicz JR, Ed.), Vol. 3, pp. 289–343, Plenum, New York.
13. Glass AM, Liao PF, Bergman JG, and Olson DH (1980) Interaction of metal particles with adsorbed dye molecules: Absorption and luminescence. Optics Letts. 5(9), 368–370.
14. Campion A, Gallo AR, Harris CB, Robota HJ, and Whitmore PM (1980) Electronic energy transfer to metal surfaces: A test of classical image dipole theory at short distances. Chem. Phys. Letts 73(3), 447–450.

15. Sokolov K, Chumanov G, and Cotton TM (1998) Enhancement of molecular fluorescence near the surface of colloidal metal films. Anal. Chem 70, 3898–3905. [PubMed: 9751028]
16. Hayakawa T, Selvan ST, and Nogami M. (1999) Field enhancement effect of small Ag particles on the fluorescence from Eu3+ -doped SiO2 glass. Appl. Phys. Lett 74(11), 1513–1515.
17. Selvan ST, Hayakawa T, and Nogami M. (1999) Remarkable influence of silver islands on the enhancement of fluorescence from Eu3+ ion-doped silica gels. J. Phys. Chem. B 103, 7064–7067.
18. Georghiou S, Nordlund TM, and Saim AM (1985) Picosecond fluorescence decay time measurements of nucleic acids at room temperature in aqueous solution. Photochem. Photobiol 41(2), 209–212.
19. Georghiou S, Bradrick TD, Philippetis A, and Beechem JM (1996) Large-amplitude picosecond anisotropy decay of the intrinsic fluorescence of double-stranded DNA. Biophys. J 70(April), 1909–1922. [PubMed: 8785350]
20. Hurtubise RJ (1990) Phosphorimetry: Theory, Instrumentation, and Applications, VCH, New York.
21. Subramaniam V, Steel DG, and Gafni A. (2000) Room temperature tryptophan phosphorescence as a probe of structural and dynamic properties of proteins In Topics in Fluorescence Spectroscopy: Protein Fluorescence (Lakowicz JR, Ed.), Vol. 6, pp. 43–65, Kluwer Academic/Plenum, New York.
22. Broos J, Strambini GB, Gonnelli M, Vos EPP, Koolhof M, and Robillard GT (2000) Sensitive monitoring of the dynamics of a membrane-bound transport protein by tryptophan phosphorescence spectroscopy. Biochemistry 39, 10877–10883. [PubMed: 10978174]
23. Daniel E, and Weber G. (1966) Cooperative effects in binding by bovine serum albumin. I. The binding of 1-anilino-8-naphthalene-sulfonate. Fluorimetric titrations. Biochemistry 5, 1893–1900. [PubMed: 5963431]
24. Slavik J. (1994) Fluorescent Probes in Cellular and Molecular Biology, Chap. 5, pp. 125–137, CRC Press, Boca Raton, FL.
25. Drexhage KH (1974) Interaction of light with monomolecular dye lasers In Progress in Optics (Wolfe E, Ed.), pp. 161–232, North-Holland, Amsterdam.
26. Amos RM, and Barnes WL (1997) Modification of the spontaneous emission rate of Eu3+ ions close to a thin metal mirror. Phys. Rev. B 55(11), 7249–7254.
27. Barnes WL (1998) Fluorescence near interfaces: The role of photonic mode density. J. Modern Optics 45(4), 661–699.
28. Amos RM, and Barnes WL (1999) Modification of spontaneous emission lifetimes in the presence of corrugated metallic surfaces. Phys. Rev. B 59(11), 7708–7714.
29. Hinds EA (1991) Cavity quantum electrodynamics. Adv. At. Mol. Opt. Phys 28, 237–289.
30. Michaels AM, Jiang J, and Brus L. (2000) Ag nanocrystal junctions as the site for surface-enhanced Raman scattering of single rhodamine 6G molecules. J. Phys. Chem. B 104, 11965–11971.
31. Freeman RG, Grabar KC, Allison KJ, Bright RM, Davis JA, Guthrie AP, Hommer MB, Jackson MA, Smith PC, Walter DG, and Natan MJ (1995) Self-assembled metal colloid monolayers: An approach to SERS substrates. Science 267, 1629–1632. [PubMed: 17808180]
32. Weitz DA, Garoff S, Hanson CD, and Gramila TJ (1982) Fluorescent lifetimes of molecules on silver-island films. Optics Letts. 7(2), 89–91.
33. Aussenegg FR, Leitner A, Lippitsch ME, Reinisch H, and Reigler M. (1987) Novel aspects of fluorescence lifetime for molecules positioned close to metal surfaces. Surface Sci. 139, 935–945.
34. Leitner A, Lippitsch ME, Draxler S, Riegler M, and Aussenegg FR (1985) Fluorescence properties of dyes absorbed to silver islands, investigated by picosecond techniques. Appl. Phys. B 36, 105–109.
35. Kerker M. (1985) The optics of colloidal silver: Something old and something new. J. Colloid Interface Sci 105, 297–314.
36. Faraday M. (1857) The Bakerian lecture. Experimental relations of gold (and other metals) to light. Philos. Trans 147, 145–181.
37. Link S, and El-Sayed MA (2000) Shape and size dependence of radiative, nonradiative and photothermal properties of gold nanocrystals. Int. Rev. Phys. Chem 19, 409–453.

38. Kreibig U, and Vollmer M. (1995) Optical Properties of Metal Clusters, Springer Series in Materials Science, Springer Verlag, Berlin.
39. Philpott MR (1975) Effect of surface plasmons on transitions in molecules. J. Chem. Phys 62(5), 1812–1817.
40. Chance RR, Prock A, and Silbey R. (1978) Molecular fluorescence and energy transfer near interfaces. Adv. Chem. Phys 37, 1–65.
41. Gersten J, and Nitzan A. (1981) Spectroscopic properties of molecules interacting with small dielectric particles. J. Chem. Phys 75(3), 1139–1152.
42. Weitz DA, Garoff S, Gersten JI, and Nitzan A. (1983) The enhancement of Raman scattering, resonance Raman scattering, and fluorescence from molecules absorbed on a rough silver surface. J. Chem. Phys 78(9), 5324–5338.
43. Chew H. (1987) Transition rates of atoms near spherical surfaces. J. Chem. Phys 87(2), 1355–1360.
44. Kummerlen J, Leitner A, Brunner H, Aussenegg FR, and Wokaun A. (1993) Enhanced dye fluorescence over silver island films: Analysis of the distance dependence. Mol. Phys 80(5), 1031–1046.
45. Garcia-Ramos JV, and Sanchez-Cortes S. (1997) Metal colloids employed in the SERS of biomolecules: Activation when exciting in the visible and near-infrared regions. J. Mol. Struct 405, 13–28.
46. Graham D, Mallinder BJ, and Smith WE (2000) Surface-enhanced resonance Raman scattering as a novel method of DNA discrimination. Angew. Chem. Int. Ed 39(6), 1061–1063.
47. Graham D, Mallinder BJ, and Smith WE (2000) Detection and identification of labeled DNA by surface enhanced resonance Raman scattering. Biopolymers 57, 85–91. [PubMed: 10766959]
48. Emory SR, and Nie S. (1998) Screening and enrichment of metal nanoparticles with novel optical properties. J. Phys. Chem. B 102, 493–497.
49. Michaels AM, Nirmal M, and Brus LE (1999) Surface enhanced raman spectroscopy of individual rhodamine 6G molecules on large Ag nanocrystals. J. Am. Chem. Soc 121, 9932–9939.
50. Sullivan KG, King O, Sigg C, and Hall DG (1994) Directional, enhanced fluorescence from molecules near a periodic surface. Appl. Optics 33(13), 2447–2454.
51. Leung PT, Kim YS, and George TF (1989) Decay of molecules at corrugated thin metal films. Phys. Rev. B 39(14), 9888–9893.
52. Kitson SC, Barnes WL, and Sambles JR (1996) Photoluminscence from dye molecules on silver gratings. Opt. Commun 122, 147–154.
53. Kitson SC, Barnes WL, Sambles JR, and Cotter NPK (1996) Excitation of molecular fluorescence via surface plasmon polaritons. J. Mod. Opt 43(3), 573–582.
54. Wokaun A, Lutz H-P, King AP, Wild UP, and Ernst RR (1983) Energy transfer in surface enhanced fluorescence. J. Chem. Phys 79(1), 509–514.
55. Ambrose WP, Goodwin PM, Jett JH, Van Orden A, Wemer JH, and Keller RA (1999) Single molecule fluorescence spectroscopy at ambient temperature. Chem. Rev 99, 2929–2956. [PubMed: 11749506]
56. Van Orden A, Machara NP, Goodwin PM, and Keller RA (1998) Single-molecule identification in flowing sample streams by fluorescence burst size and intraburst fluorescence decay rate. Anal. Chem 70(7), 1444–1451. [PubMed: 21644740]
57. Soper SA, Nutter HL, Keller RA, Davis LM, and Shera EB (1993) The photophysical constants of several fluorescent dyes pertaining to ultrasensitive fluorescence spectroscopy. Photochem. Photobiol 57(6), 972–977.
58. Kirsch AK, Subramaniam V, Jenei A, and Jovin TM (1999) Fluorescence resonance energy transfer detected by scanning near-field optical microscopy. J. Microsc 194, 448–454. [PubMed: 10999315]
59. Garoff S, Weitz DA, Alvarez MS, and Gersten JI (1984) Electrodynamics at rough metal surfaces: Photochemistry and luminescence of adsorbates near metal-island films. J. Chem. Phys 81(11), 5189–5200.

60. Eftink MR (1991) Fluorescence quenching reactions: Probing biological macromolecular structures In Biophysical and Biochemical Aspects of Fluorescence Spectroscopy (Dewey TG, Ed.), pp. 1–41, Plenum, New York.
61. Eftink MR (1991) Fluorescence quenching: Theory and applications In Topics in Fluorescence Spectroscopy: Principles (Lakowicz JR, Ed.), Vol. 2, pp. 53–126, Plenum, New York.
62. van den Berg PAW, van Hoek A, Walentas CD, Perham RN, and Visser AJWG (1998) Flavin fluorescence dynamics and photoinduced electron transfer in Escherichia coli glutathione reductase. Biophys. J 74, 2046–2058. [PubMed: 9545063]
63. Visser AJ, Ghisla S, Massey V, Muller F, and Veeger C. (1979) Fluorescence properties of reduced flavins and flavoproteins. Eur. J. Biochem 101(1), 13–21. [PubMed: 510300]
64. Albani JR, Sillen A, Engelborghs Y, and Gervais M. (1999) Dynamics of flavin in flavocytochrome b2: A fluorescence study. Photochem. Photobiol 69(1), 22–26.
65. Swadesh JK, Mui PW, and Scheraga HA (1987) Thermodynamics of the quenching of tyrosyl fluorescence by dithiothreitol. Biochemistry 26, 5761–5769. [PubMed: 3676287]
66. Loewenthal R, Sancho J, and Fersht AR (1991) Fluorescence spectrum of barnase: Contributions of three tryptophan residues and a histidine-related pH dependence. Biochemistry 30, 6775–6779. [PubMed: 2065058]
67. Rouviere N, Vincent M, Craescu CT, and Gallay J. (1997) Immunosuppressor binding to the immunophilin FKBP59 affects the local structural dynamics of a surface β-strand: Time-resolved fluorescence study. Biochemistry 36, 7339–7352. [PubMed: 9200682]
68. Georghiou S, Nordlund TM, and Saim AM (1985) Picosecond fluorescence decay time measurements of nucleic acids at room temperature in aqueous solution. Photochem. Photobiol 41(2), 209–212.
69. Plessow R, Brockhinke A, Eimer W, and Kohse-Hoinghaus K. (2000) Intrinsic time-and wavelength-resolved fluorescence of oligonucleotides: A systematic investigation using a novel picosecond laser approach. J. Phys. Chem 104, 3695–3704.
70. Easter JH, DeToma RP, and Brand L. (1978) Fluorescence measurements of environmental relaxation at the lipid–water interface region of bilayer membranes. Biochim. Biophys. Acta 508, 27–38. [PubMed: 629967]
71. Lakowicz JR, Cherek H, Laczko G, and Gratton E. (1984) Time-resolved fluorescence emission spectra of labeled phospholipid vesicles, as observed using multifrequency phase-modulation fluorometry. Biochim. Biophys. Acta 777, 183–193.
72. Brand L, and Gohike JR (1971) Nanosecond time-resolved fluorescence spectra of a protein–dye complex. J. Biol. Chem 246, 2317–2324. [PubMed: 5103072]
73. Gafni A, DeToma RP, Manrow RE, and Brand L. (1977) Nanosecond decay studies of a fluorescence probe bound to apomyoglobin. Biophys. J 17, 155–168. [PubMed: 836933]
74. Weber G, and Farris FJ (1979) Synthesis and spectral properties of a hydrophobic fluorescent probe: 6-Propionyl-2(dimethyl-amino) naphthalene. Biochemistry 18, 3075–3078. [PubMed: 465454]
75. Predergast FG, Meyer M, Carlson GL, Iida S, and Potter JD (1983) Synthesis, spectral properties, and use of 6-acryloyl-20-dimethylaminonaphthalene (acrylodan). J. Biol. Chem 258, 7541–7544. [PubMed: 6408077]
76. Gersten JI, and Nitzan A. (1984) Accelerated energy transfer between molecules near a solid particle. Chem. Phys. Letts 104(1), 31–37.
77. Hua XM, Gersten JI, and Nitzan A. (1985) Theory of energy transfer between molecules near solid state particles. J. Chem. Phys 83, 3650–3659.
78. Lakowicz JR (1999) Principles of Fluorescence Spectroscopy, 2nd ed., Kluwer Academic/Plenum, New York.
79. Fisz JJ (1996) Polarized fluorescence decay surface for a mixture of non-interacting species in solution. Chem. Phys. Lett 259, 579–587.
80. Bialik CN, Wolf B, Rachofsky EL, Ross JBA, and Laws WR (1998) Fluorescence anisotropy decay: Finding the correct physical model. Proc. SPIE 3256, 60–67.
81. Thompson TE, Sankaram MB, Biltonen RL, Marsh D, and Vaz WLC (1995) Effects of domain structure on in-plane reactions and interactions. Mol. Mem. Biol 12, 157–162.

82. Edidin M. (1997) Lipid microdomains in cell surface membranes. Curr. Opin. Struct. Biol 4(7), 528–532.

83. Hamann HF, Gallagher A, and Nesbitt DJ (2000) Nearfield fluorescence imaging by localized field enhancement near a sharp probe tip. Chem. Phys. Lipids 76, 1953–1955.

84. Pagnot T, Barchiesi D, Van Labeke D, and Pieralli C. (1997) Use of a scanning near-field optical microscope architecture to study fluorescence and energy transfer near a metal. Opt. Letts 22(2), 120–122. [PubMed: 18183122]

85. Hayazawa N, Inouye Y, and Kawata S. (1999) Evanescent field excitation and measurement of dye fluorescence in a metallic probe near-field scanning optical microscope. J. Microsc 194(2/3), 472–476. [PubMed: 11388288]

86. Pagnot T, Barchiesi D, and Tribillon G. (1999) Energy transfer from fluorescent thin films to metals in near-field optical microscopy: Comparison between time-resolved and intensity measurements. Appl. Phys. Letts 75, 4207–4209.

87. Garcia-Parajo MF, Veerman J-A, Segers-Nolten GMJ, de Grooth BG, Greve J, and van Hulst NF (1999) Visualising individual green fluorescent proteins with a near-field microscope. Cytometry 36, 239–246. [PubMed: 10404974]

88. Veerman JA, Levi SA, van Veggel FCJM, Reinhoudt DN, and van Hulst NF (1999) Near-field scanning optical microscopy of single fluorescent dendritic molecules. J. Phys. Chem. A 103, 11264–11270.

89. van Hulst NF, Veerman J-A, Garcia-Parajo MF, and Kulpers L. (2000) Analysis of individual (macro) molecules and proteins using near-field optics. J. Chem. Phys 112(18), 7799–7810.

90. Vickery SA, and Dunn RC (1999) Scanning near-field fluorescence resonance energy transfer microscopy. Biophys. J 76, 1812–1818. [PubMed: 10096880]

91. Sekatskii SK, Shubeita G. t., Chergui M, Dietler G, Mironov BN, Lapshin DA, and Letokhov VS (2000) Towards the fluorescence resonance energy transfer (FRET) scanning near-field optical microscopy: Investigation of nanolocal FRET processes and FRET probe microscope. J. Exp. Theor. Phys 90, 769–777.

92. Brunner R, Bietsch A, Hollricher O, Marti O, and Lambacher A. (1997) Application of a near-field optical microscope to investigate the fluorescence energy transfer between chromophores embedded in Langmuir–Blodgett films. Surface Intern. Anal 25, 492–495.

93. Schalkhammer T, Aussenegg FR, Leitner A, Brunner H, Hawa G, Lobmaier C, and Pittner F. (1997) Detection of fluorophore-labelled antibodies by surface-enhanced fluorescence on metal nanoislands. SPIE 2976, 129–136.

94. Mayer C, Stich N, and Schalkhammer TGM (2001) Surface-enhanced fluorescence biochips using industrial standard slide format and scanners. SPIE, in press.

95. Albert KJ, Lewis NS, Schauer CL, Sotzing GA, Stitzel SE, Vaid TP, and Walt DR (2000) Cross-reactive chemical sensor arrays. Chem. Rev 100, 2595–2626. [PubMed: 11749297]

96. Feldstein MJ, Golden JP, Rowe CA, MacCraith BD, and Ligler FS (1999) Array biosensor: Optical and fluidics systems. J. Biomed. Microdevices 1, 139–153.

97. Li L, Ruzgas T, and Gaigalas AK (1999) Fluorescence from alexa 488 fluorophore immobilized on a modified gold electrode. Langmuir 15, 6358–6363.

98. Ullman EF, Schwarzberg M, and Rubenstein KE (1976) Fluorescent excitation transfer immunoassay: A general method for determination of antigens. J. Biol. Chem 251(14), 4172–4178. [PubMed: 945272]

99. Ozinskas AJ, Malak H, Joshi J, Szmacinski H, Britz J, Thompson RB, Koen PA, and Lakowicz JR (1993) Homogeneous model immunoassay of thyroxine by phase-modulation fluorescence spectroscopy. Anal. Biochem 213, 264–270. [PubMed: 8238900]

100. Benner RE, Dornhaus R, and Chang RK (1979) Angular emission profiles of dye molecules excited by surface plasmon waves at a metal surface. Opt. Commun 30(2), 145–149.

101. Kano H, and Kawata S. (1996) Two-photon excited fluorescence enhanced by a surface plasmon. Opt. Letts 21(22), 1848–1850. [PubMed: 19881822]

102. McCord P, and Bard AJ (1991) Electrogenerated chemiluminescence. J. Electroanal. Chem 318, 91–99.

103. Miller CJ, McCord P, and Bard AJ (1991) Study of Langmuir monolayers of ruthenium complexes and their aggregation by electrogenerated chemiluminescence. Langmuir 7, 2781–2787.
104. Blackburn GF, Shah HP, Kenten JH, Leland J, Kamin R. a., Link J, Peterman J, Powell MJ, Shah A, Talley DB, Tyagi SK, Wilkins E, Wu T-G, and Massey RJ (1991) Electrochemiluminescence detection for development of immunoassays and DNA probe assays for clinical diagnosis. Clin. Chem 37, 1534–1539. [PubMed: 1716534]
105. Ferea TL, and Brown PO (1999) Observing the living genome. Curr. Opin. Genet. Dev 9, 715–722. [PubMed: 10607618]
106. Gatto-Menking DL, Yu H, Bruno JG, Goode MT, Miller M, and Zulich AW (1995) Sensitive detection of biotoxoids and bacterial spores using an immunomagnetic electrochemiluminescence sensor. Biosens. Bioelectron 10, 501–507. [PubMed: 7612203]
107. Lipschutz RJ, Fodor SPA, Gingeras TR, and Lockhart DJ (1999) High density synthetic olionucleotide arrays. Nat. Genet. Suppl 1(1), 20–24.
108. Harrington CA, Rosenow C, and Retief J. (2000) Monitoring gene expression using DNA microarrays. Curr. Opin. Microbiol 3, 285–291. [PubMed: 10851158]
109. Morrison LE (1995) Detection of energy transfer and fluorescence quenching In Nonisotopic Probing, Blotting, and Sequencing (Kricka LJ, Ed.), pp. 429–471, Academic Press, New York.
110. Parkhurst KM, and Parkhurst LJ (1996) Detection of point mutations in DNA by fluorescence energy transfer. J. Biomed. Opt 1(4), 435–441. [PubMed: 23014787]
111. Gersten JI, and Nitzan A. (1985) Photophysics and photochemistry near surfaces and small particles. Surface Sci. 158, 165–189.
112. (2001) The human genome. Nature February 15, 813–958.
113. (2001) The human genome. Science February 16, 1177–1351.
114. Enderlein J, Robbins DL, Ambrose WP, and Keller RA (1998) Molecular shot noise, burst size distribution, and single-molecule detection in fluid flow: Effects of multiple occupancy. J. Phys. Chem. A 102, 6089–6094.
115. Van Orden A, Machara NP, Goodwin PM, and Keller RA (1998) Single-molecule identification in flowing sample streams by fluorescence burst size and intraburst fluorescence decay rate. Anal. Chem 70(7), 1444–1451. [PubMed: 21644740]
116. Garcia-Ramos JV, and Sanches-Cortes S. (1997) Metal colloids employed in the SERS of biomolecules: Activation when exciting in the visible and near-infrared regions. J. Mol. Struct 405, 13–28.
117. Jensen TR, Malinsky MD, Haynes CL, and Van Duyne RP (2000) Nanosphere lithography: Tunable localized surface plasmon resonance spectra of nanoparticles. J. Phys. Chem. B 104, 10549–10556.
118. Malinsky MD, Kelly KL, Schatz GC, and Van Duyne RP (2001) Chain length dependence and sensing capabilities of the localized surface plasmon resonance of silver nanoparticles chemically modified with alkanethiol self-assembled monolayers. J. Am. Chem. Soc 123, 1471–1482.
119. Eck D, Helm CA, Wagner NJ, and Vaynberg KA (2001) Plasmon resonance measurements of the adsorption and adsorption kinetics of a biopolymer onto gold nanocolloids. Langmuir 17(4), 957–960.
120. Valina-Saba M, Bauer G, Stich N, Pittner F, and Schalkhammer T. (1999) A self-assembled shell of 11-mercaptoundecanoic aminophenylboronic acids on gold nanoclusters. Mat. Sci. Eng. C 8–9, 205–209.

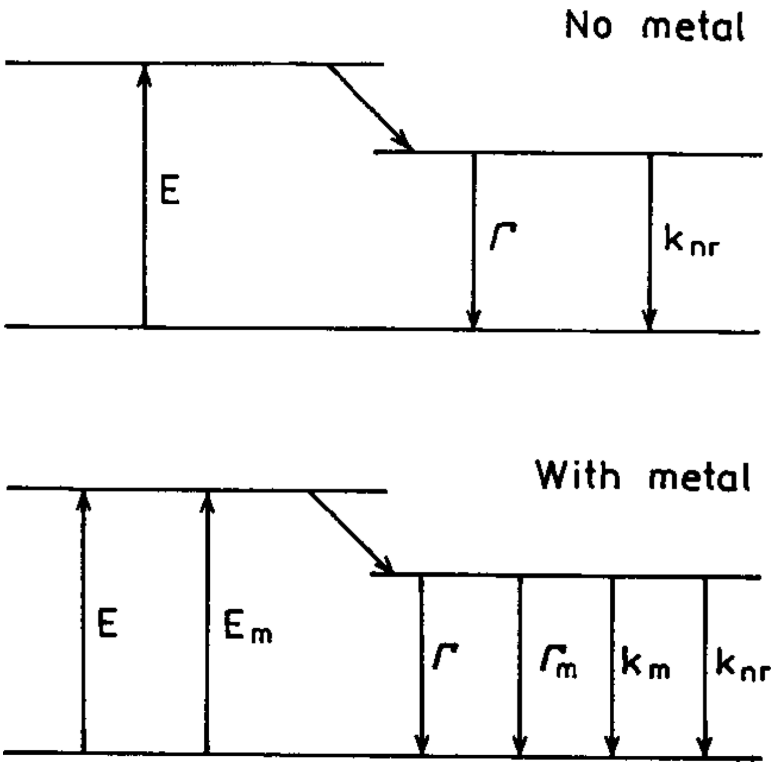

FIG. 1.

Jablonski diagram without (top) and with (bottom) the effects of near metal surfaces. For distances over 50 Å the effect of quenching by the metal (k_m) is expected to be minimal.

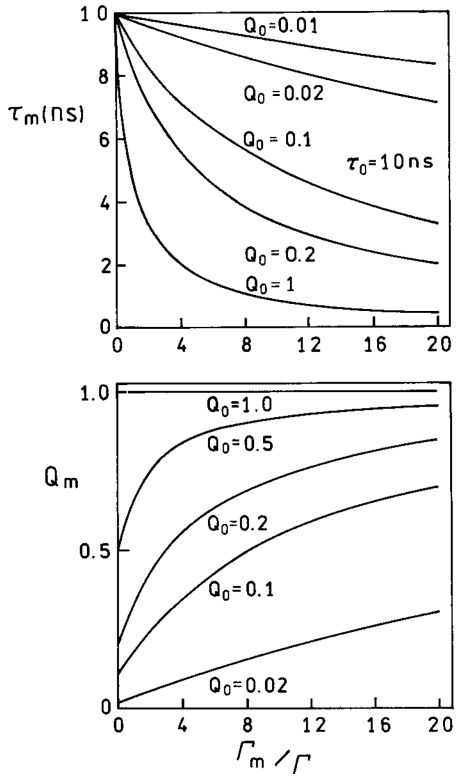

FIG. 2.

Effect of an increase in the metal-induced radiative rate on the lifetime and quantum yields of fluorophores. To clarify this figure we note that for $Q = 0.5$, $\Gamma = 5 \times 10^7$/s and $k_{nr} = 5 \times 10^7$ s. For $Q = 0.1$, $\Gamma = 1 \times 10^7 =$ s and $k_{nr} = 9 \times 10^7$ s.

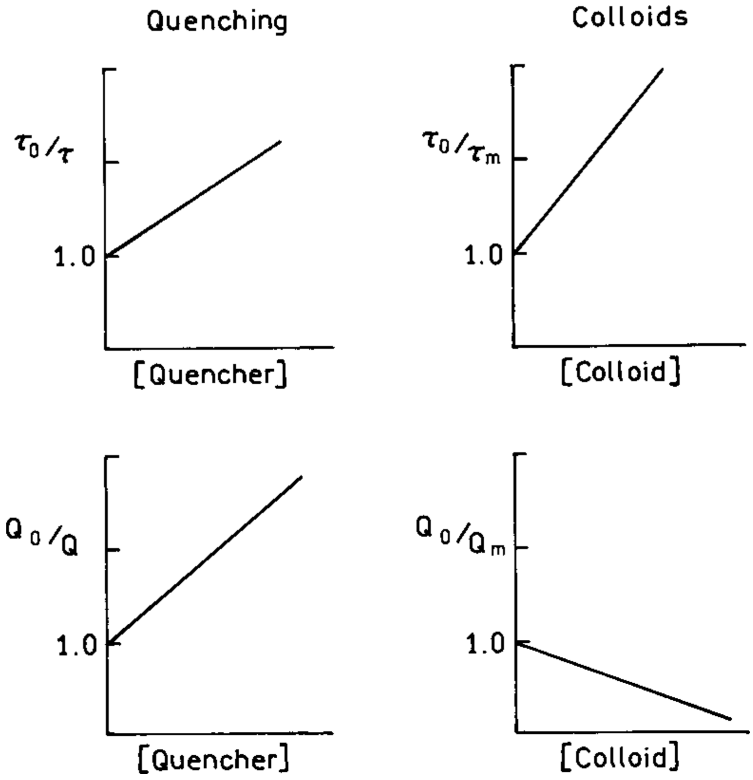

FIG. 3.

Comparison of Stern–Volmer plots for collisional quenching and colloids which enhance Γ_m.

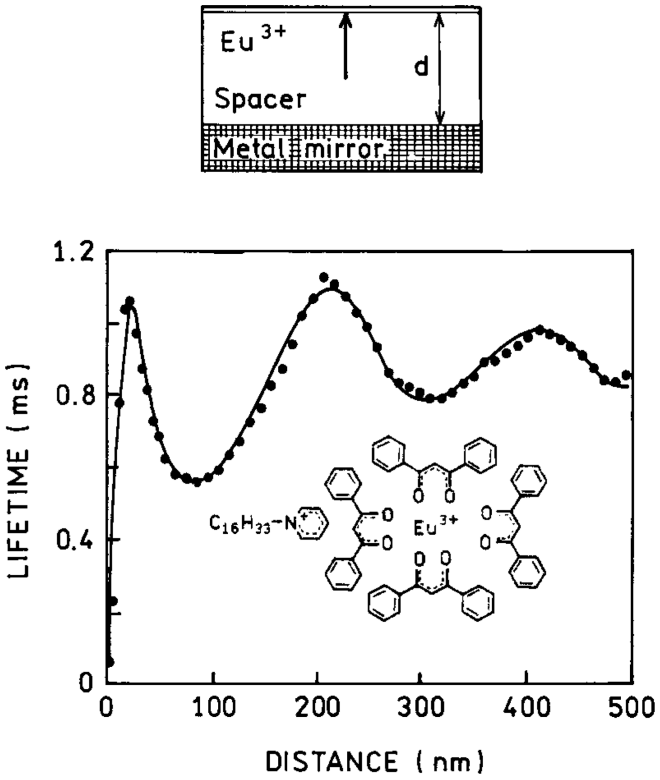

FIG. 4.

Lifetime of Eu^{3+} ions in front of a Ag mirror as a function of separation between the Eu^{3+} ions and the mirror. The solid curve is a theoretical fit.

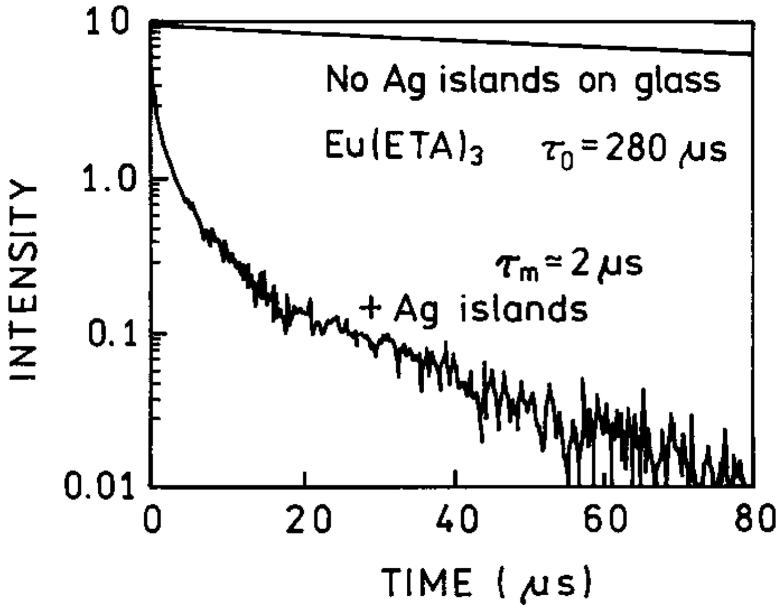

FIG. 5.

Fluorescence decay of $Eu(ETA)_3$ on silver-island films. Eu^{3+} was complexed with thenolytrifluoroacetonate (ETA).

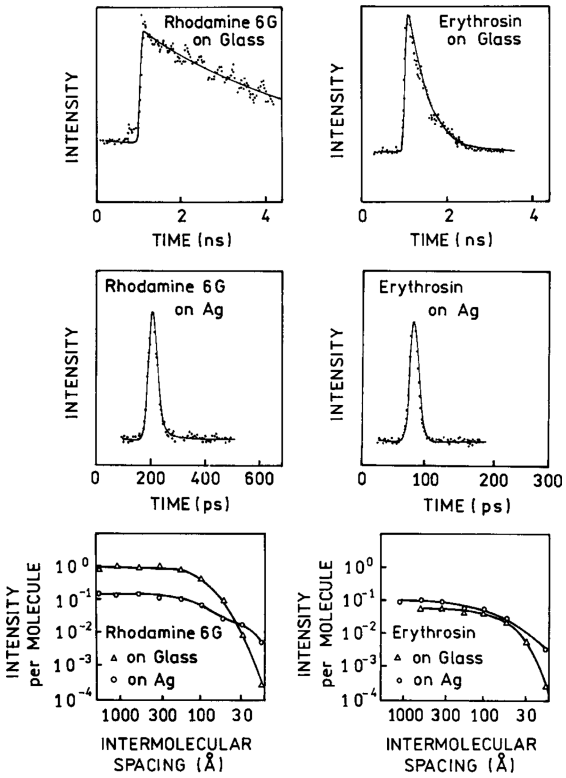

FIG. 6.

Intensity decays of rhodamine 6G and erythrosin on pure glass or silver islands. The lower panel shows how the intensity per molecule and lifetime depends on the surface density of the fluorophore.

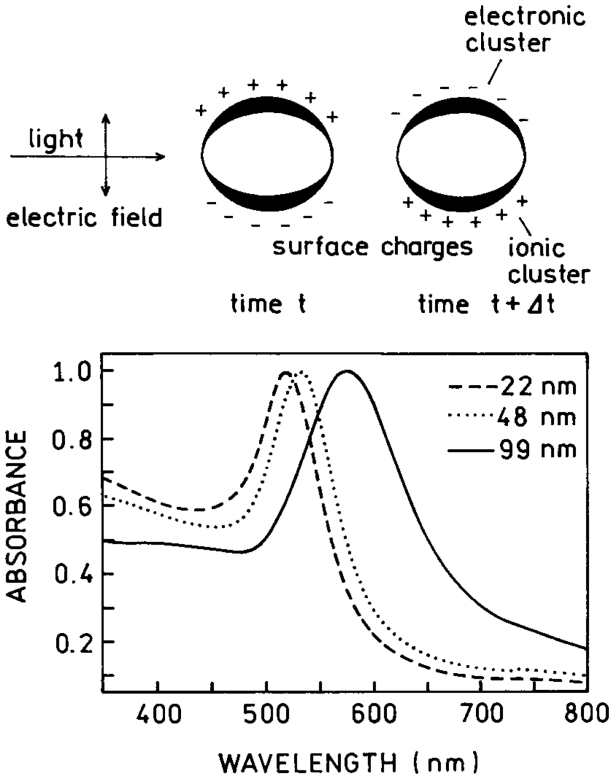

FIG. 7.
Absorption spectra of gold colloidal spheres.

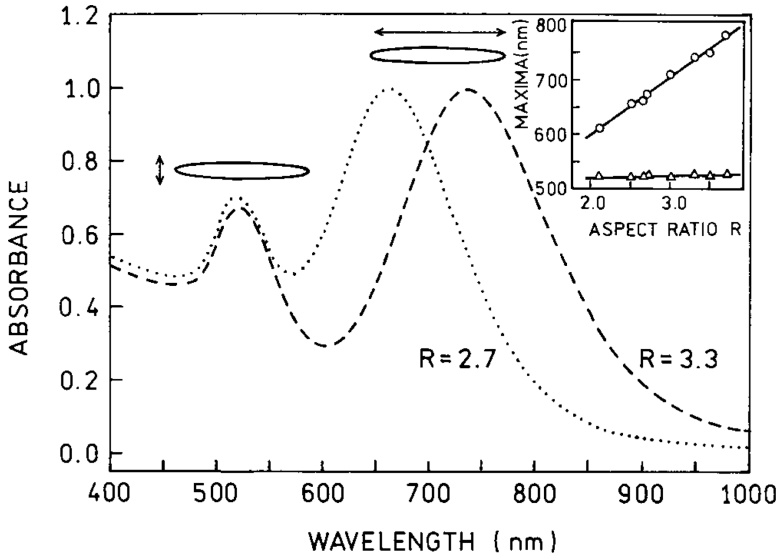

FIG. 8.
Absorption spectra of gold spheroids.

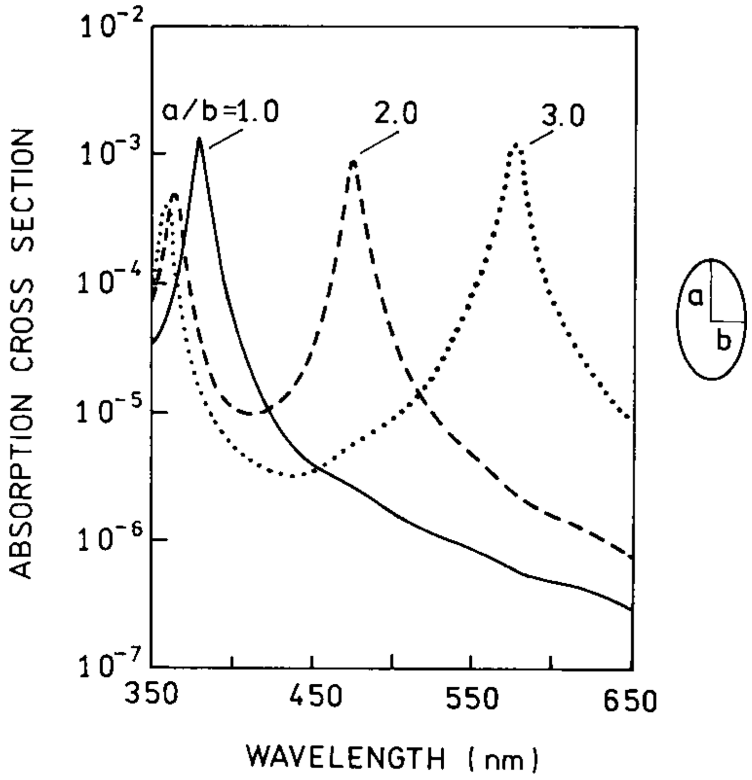

FIG. 9.

Calculated absorption cross section for a silver sphere in water (—) and for prolate spheroids with axial ratios of 2.0 and 3.0 in the small particle limit.

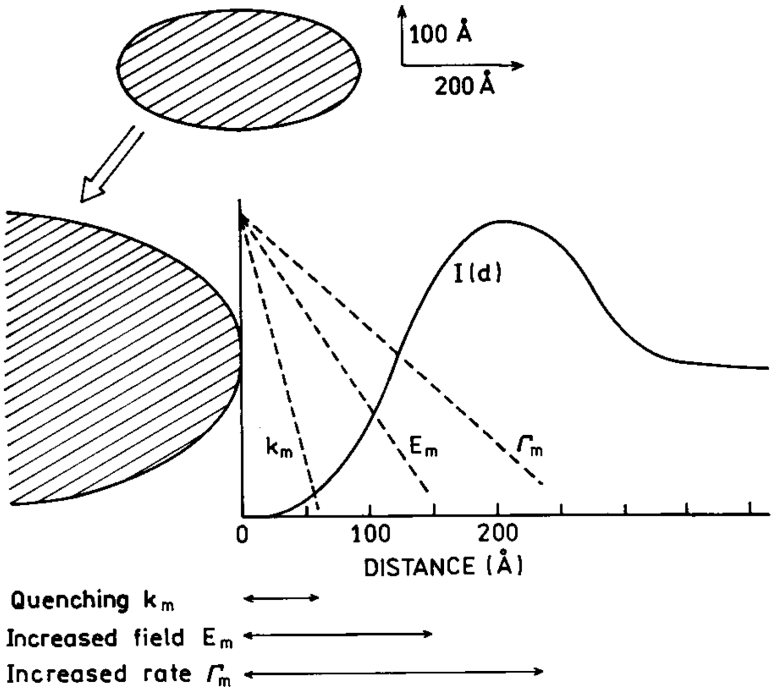

FIG. 10.

Effects of a metallic particle on transitions of a fluorophore. Metallic particles can cause quenching (k_{nr}), can concentrate the incident light field (E_m), and can increase the radiative decay rate (Γ_m).

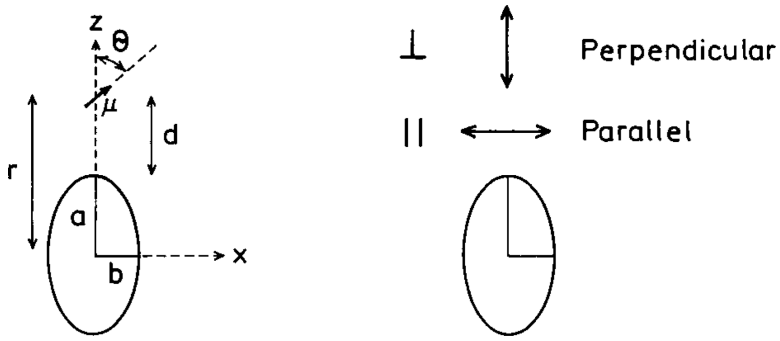

FIG. 11.
Fluorophore near a metallic spheroid.

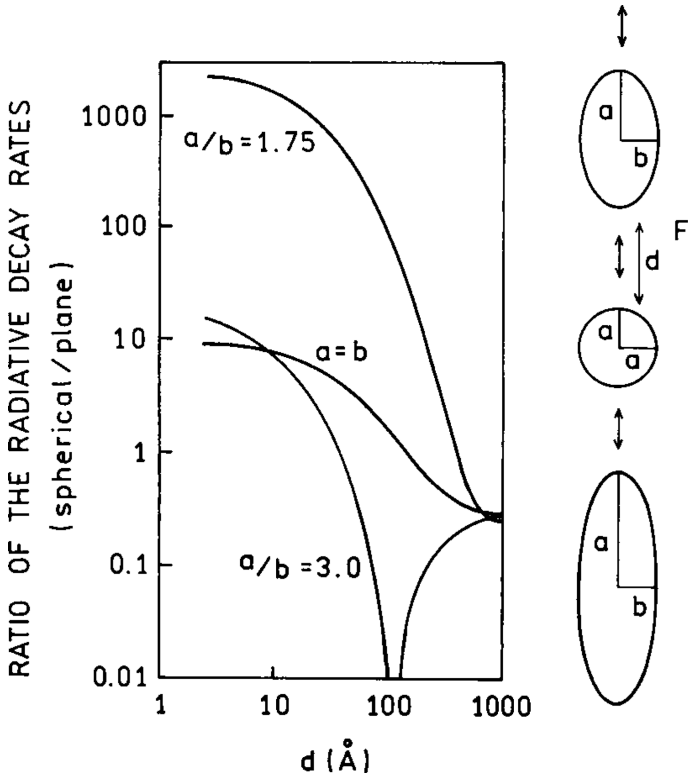

FIG. 12.

Effect of a metallic spheroid on the radiative decay rate of a fluorophore. The resonant frequency of the dye is assumed to be 25,600 cm^{-1}, approximately equal to 391 nm. The volume of the spheroids is equal to that of a sphere with a radius of 200 Å.

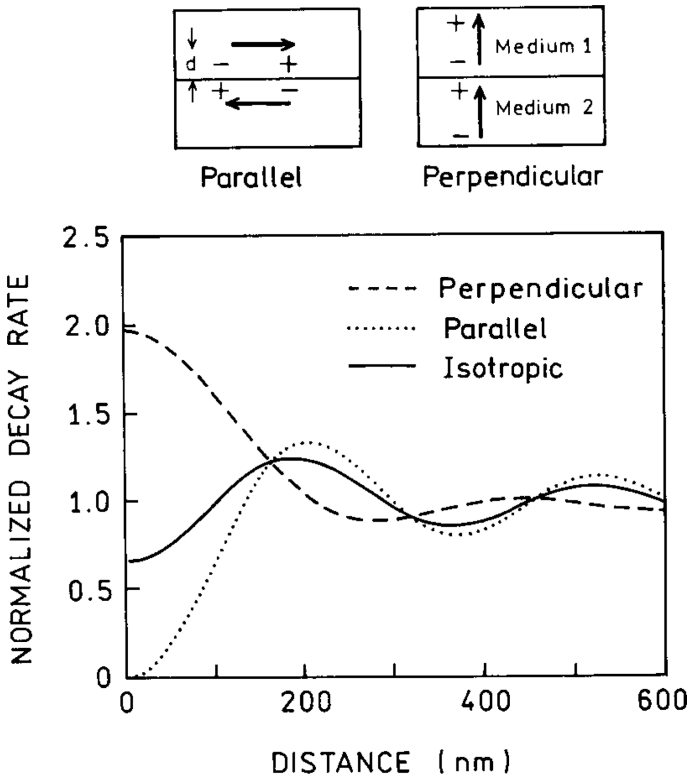

FIG. 13.
Effect of fluorophore orientation on the decay rate of a fluorophore near a metallic surface.

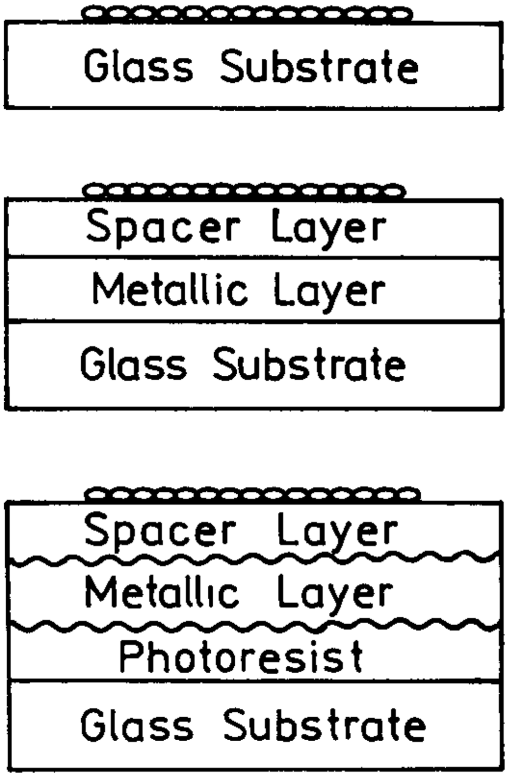

FIG. 14.

Sample configurations: top, rhodamine B on a glass slide; middle, slide with a 200-nm-thick layer of silver and a LiF dielectric spacer; bottom, the metallic layer is periodic with $d = 300$ nm due to a layer of photoresist.

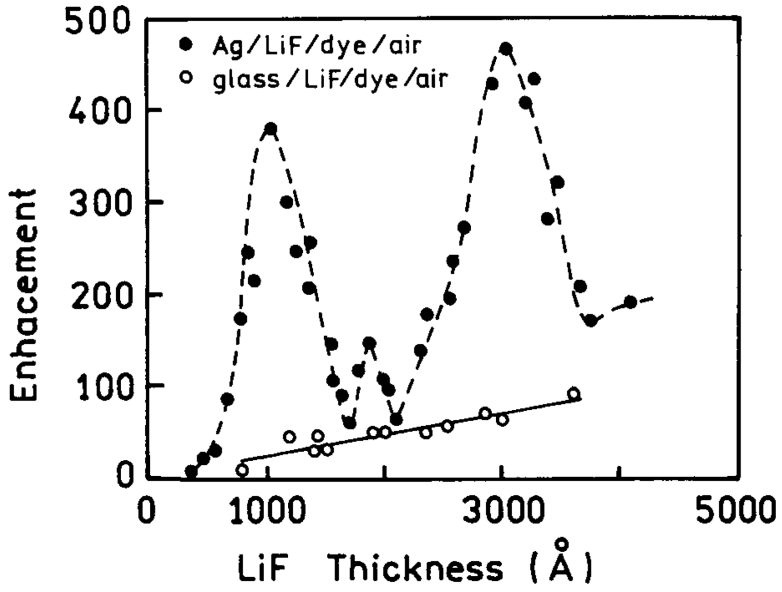

FIG. 15.

Measured enhancement versus the LiF layer thickness for the periodic metal surface (●) and for the glass/LiF/dye/air structure (◯).

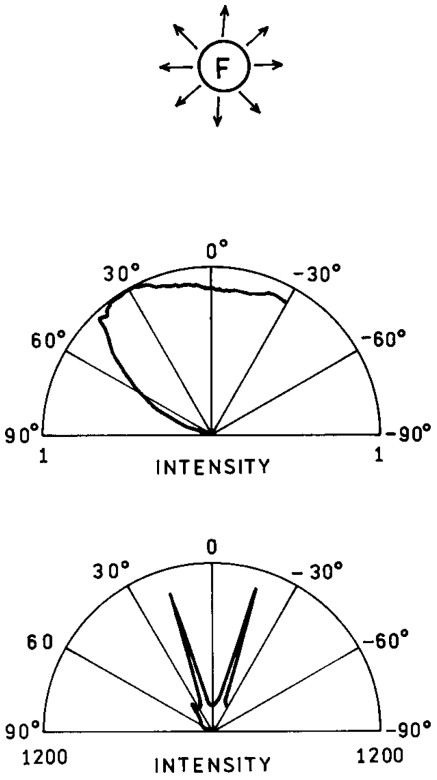

FIG. 16.

Directional emission from fluorophores near a plane (top) or periodic surface (bottom). The lower panel is for the TE-polarized emission. In the absence of a metal surface the emission is essentially isotropic (top). Note that the scales are different for the middle and lower panels.

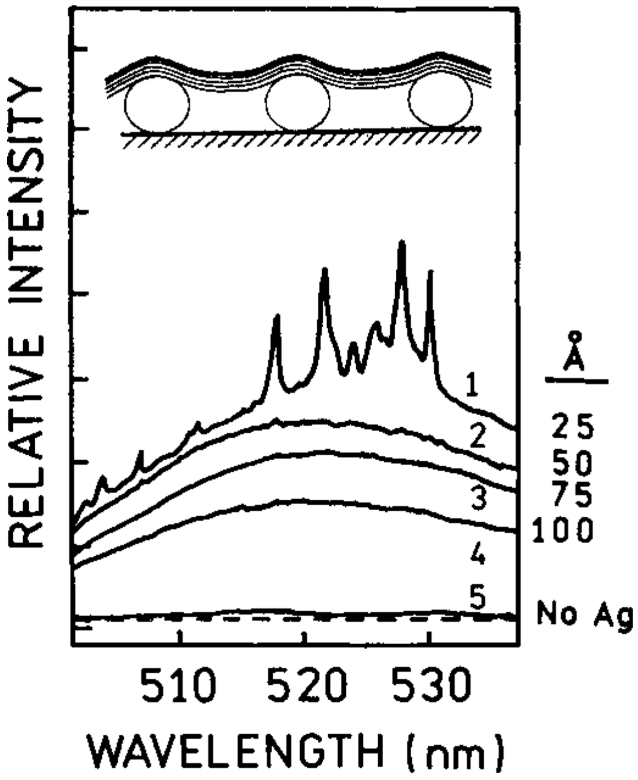

FIG. 17.

Emission spectra of mixed monolayers of fluorescein-labeled phospholipid (FIPPE)/ phospholipid (DPPE) with mole ratio 1:3 for different numbers of octadecanoic acid spacer layers (2.5 nm thick) on (1) mixed monolayer directly transferred on a colloidal film; (2) one spacer layer; (3) three spacer layers; (4) five spacer layers; and (5) mixed monolayer with three spacer layers on a bare glass slide. The dashed line represents the instrument background. The spectra were taken with 488.0-nm laser excitation. The inset shows the sample configuration.

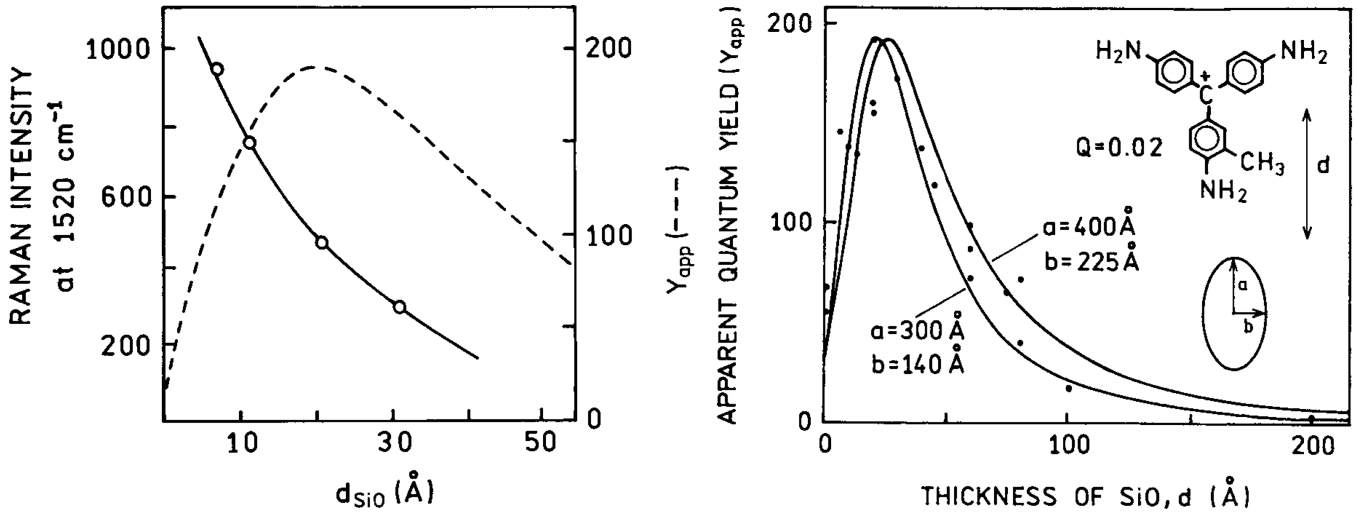

FIG. 18.

Apparent yield Y_{app} vs thickness of SiOx spacer layer from 0.1 monolayers of basic Fuchsin on a 40-Å Ag island film. The apparent yield is defined as the emission intensity relative to the intensity from molecules on an inert substrate, at constant incident power and for the same dye coverage. The filled circles are experimental data; the full lines show the results of calculations for the indicated ellipsoid dimensions. The chromophore basic Fuchsin is shown as an inset. The open circles in the left panel show the effect of distance on the Raman scattering intensity. This effect decreases more rapidly with distance than surface-enhanced fluorescence.

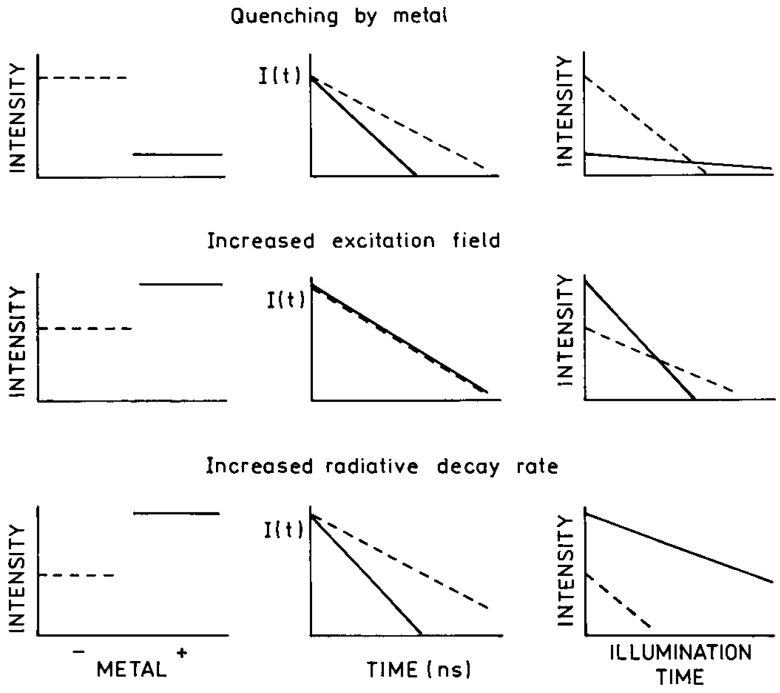

FIG. 19.

Effects of metals on the steady-state intensity, intensity decay, and photobleaching of a nearby fluorophore. From top to bottom the panels show quenching by the metal, the effect of an increased excitation field, and the effects of an increased radiative decay rate. The dashed lines indicate the absence of metal and the solid line indicates the presence of metal.

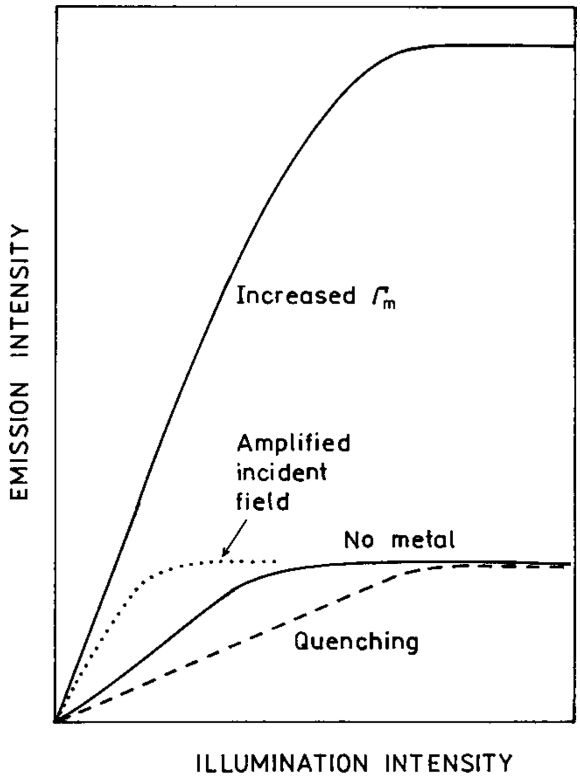

FIG. 20.

Effect of illumination intensity on a fluorophore in free space and affected by a metal surface excited by the amplified intensity, or with an increased radiative decay rate.

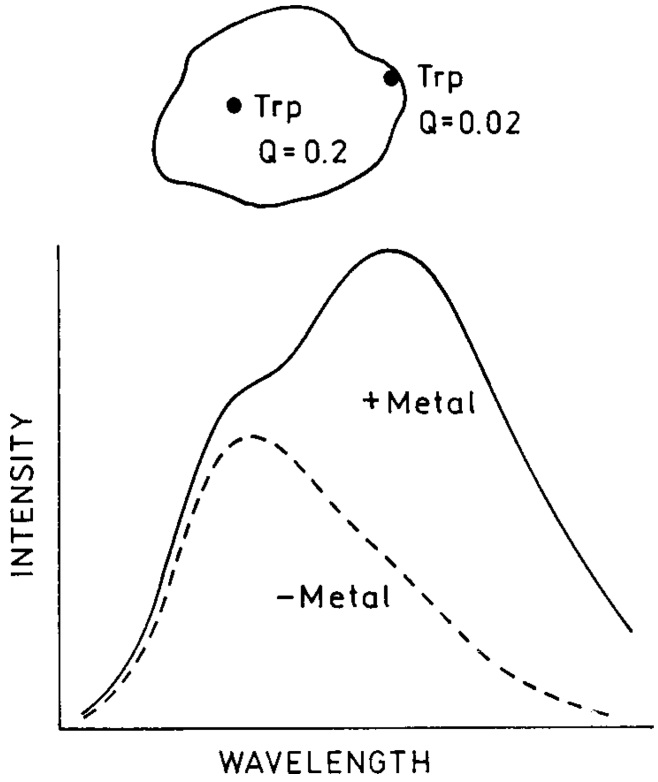

FIG. 21.

Effect of an increased radiative rate on a protein with two tryptophan residues, one of which has a low quantum yield.

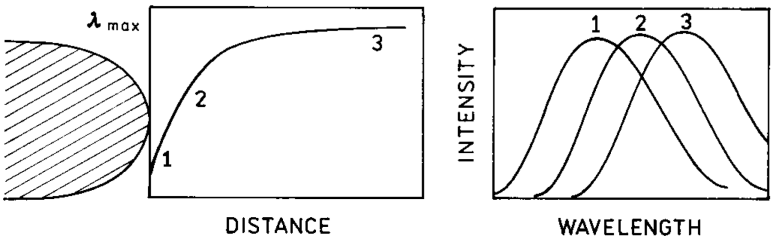

FIG. 22.

Effect of an increased radiative decay rate on the emission spectra of a polarity-sensitive fluorophore.

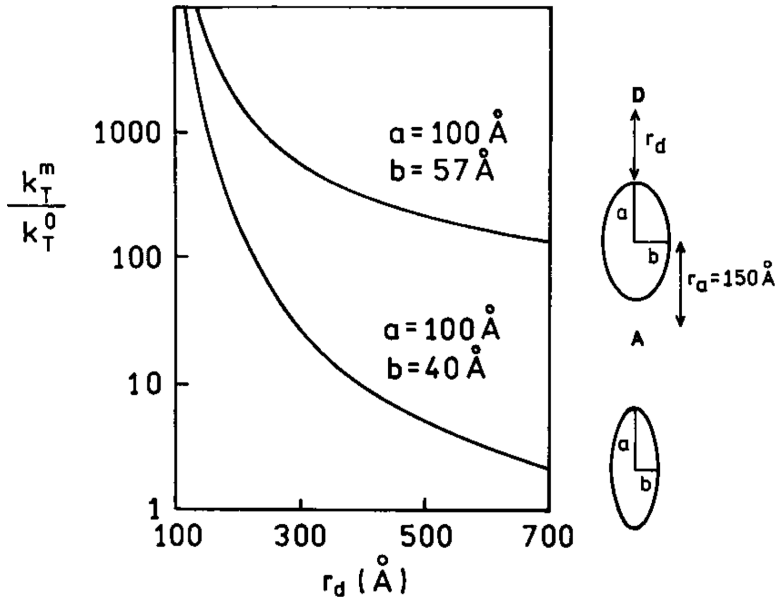

FIG. 23.

Enhancements in the rate of energy transfer in the presence of a silver particle.

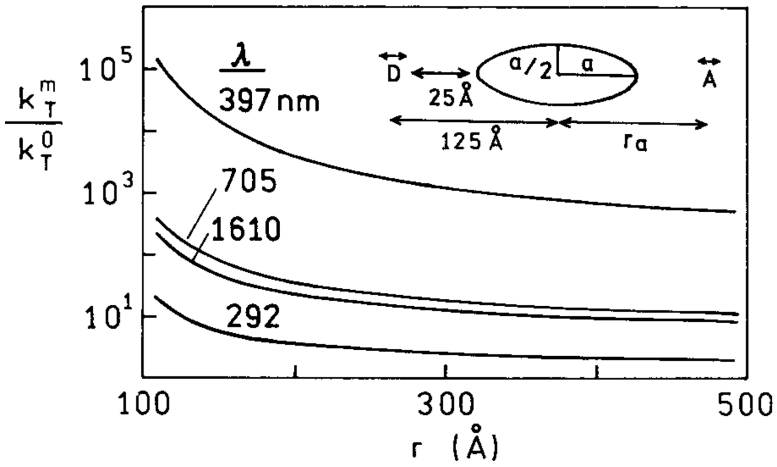

FIG. 24.

Effect of particle size on the enhancement of energy transfer. In this figure *a* is 100 Å and r_a is the distance from the center of the ellipsoid. The *D* and *A* transition moments are parallel to the long axis of the ellipsoid.

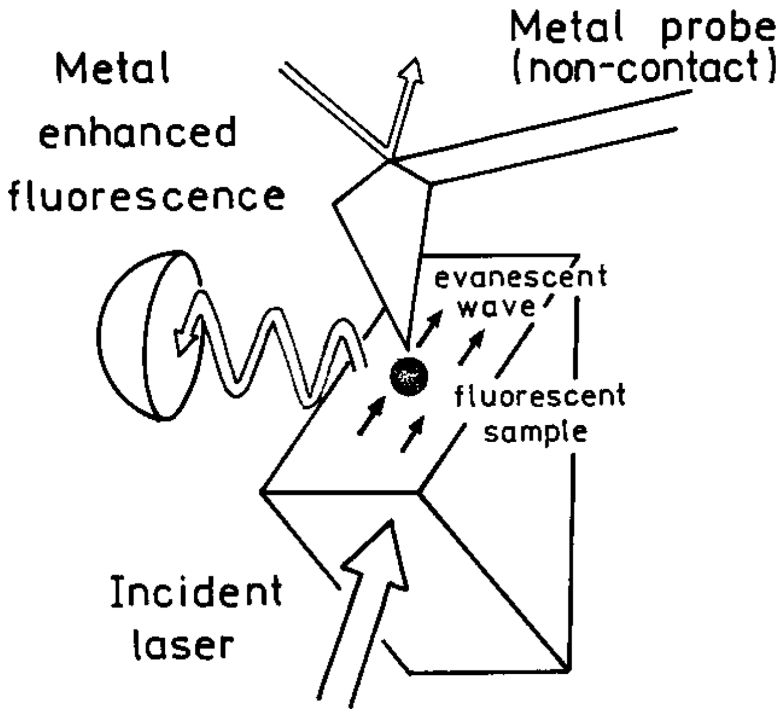

FIG. 25.
Use of metal-enhanced fluorescence in near-field microscopy.

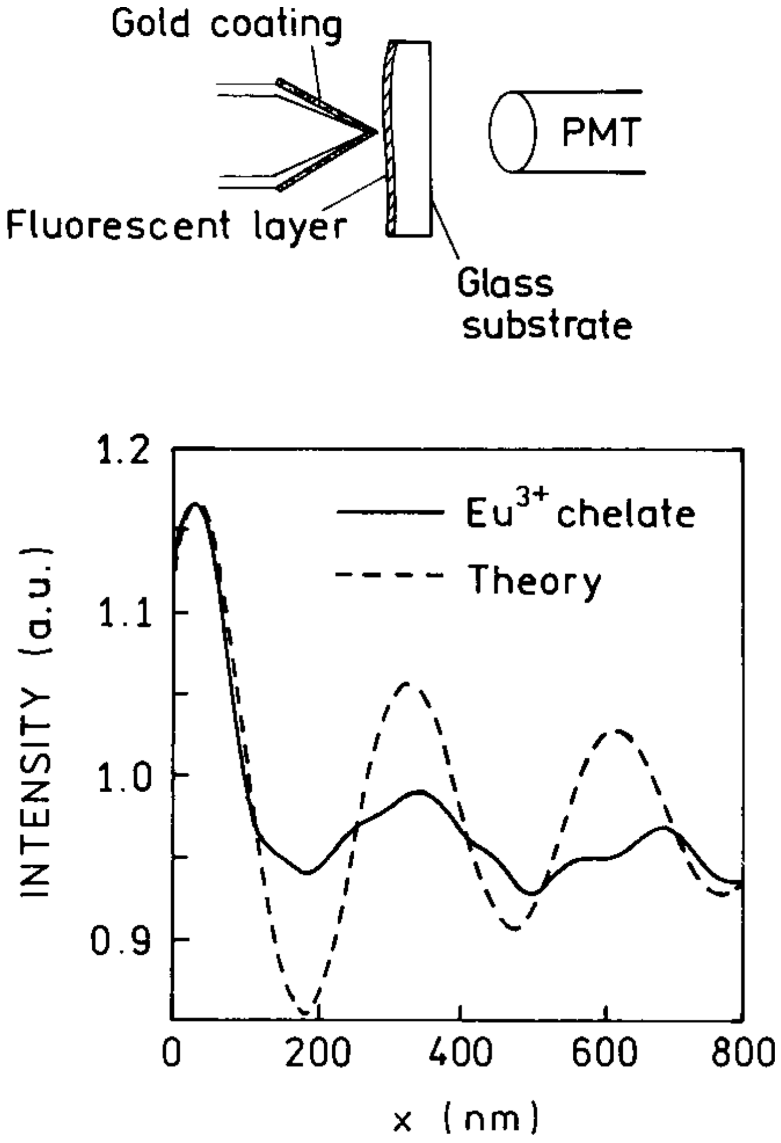

FIG. 26.
Effect of distance between the sample and a gold AFM tip on.

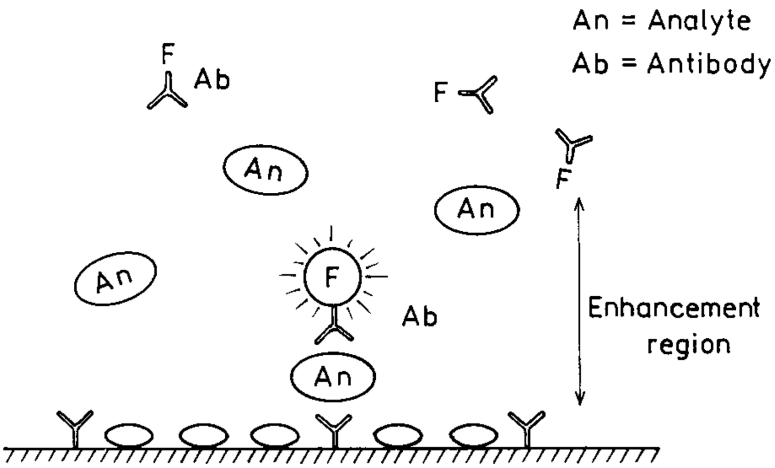

FIG. 27.
Sandwich immunoassay with low quantum yield fluorophores.

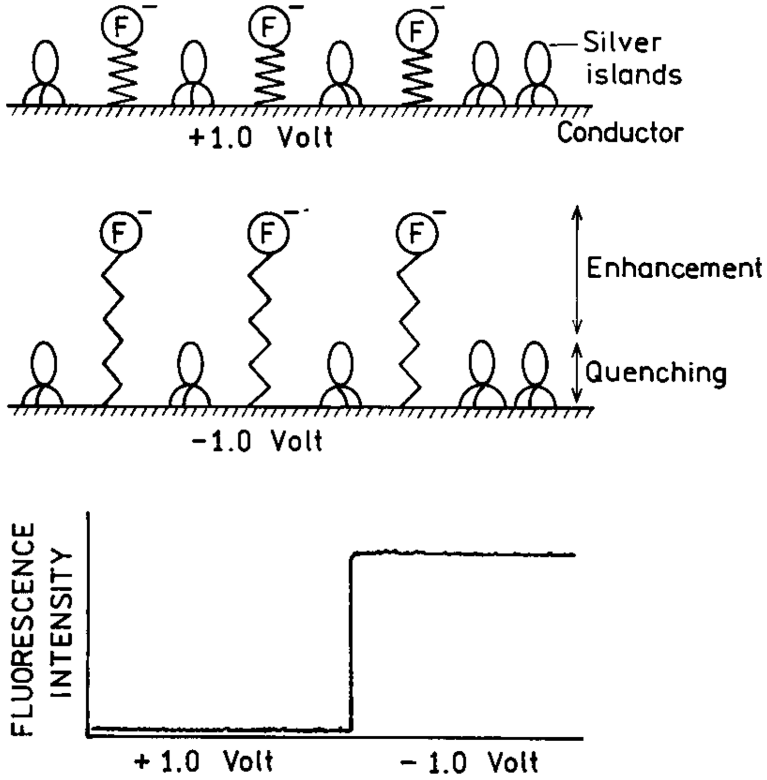

FIG. 28.
Voltage-activated fluorescence assays based on metal effects.

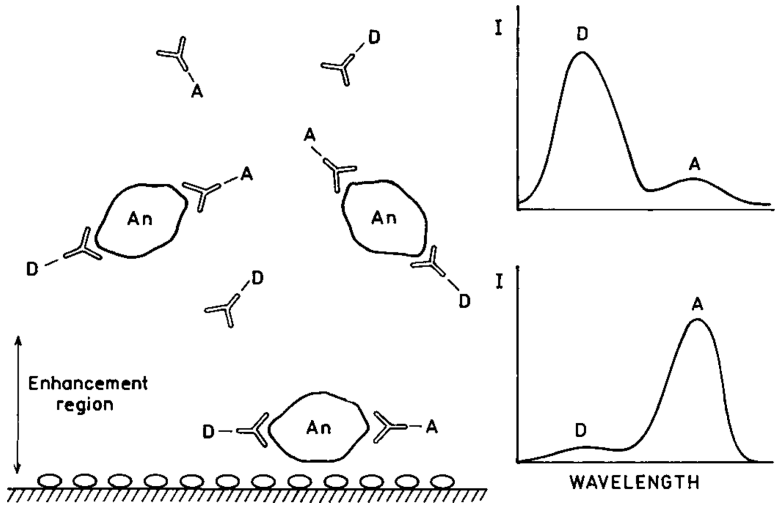

FIG. 29.
Energy transfer immunoassay using donor- and acceptor-labeled antibodies.

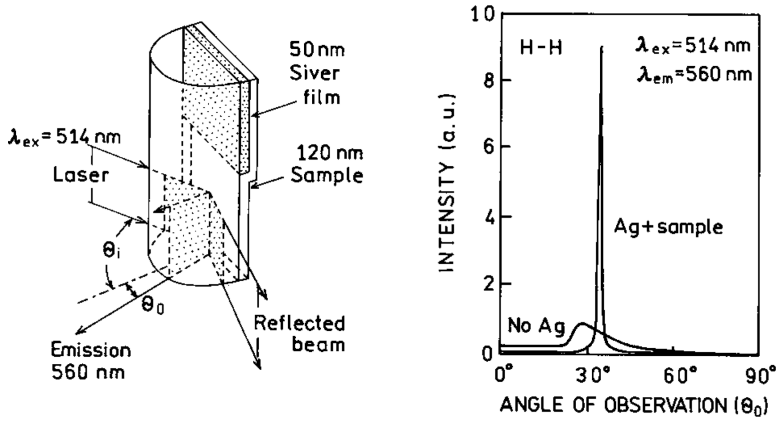

FIG. 30.

Apparatus for surface plasmon excitation and angular distribution of the fluorescence from rhodamine 6G.

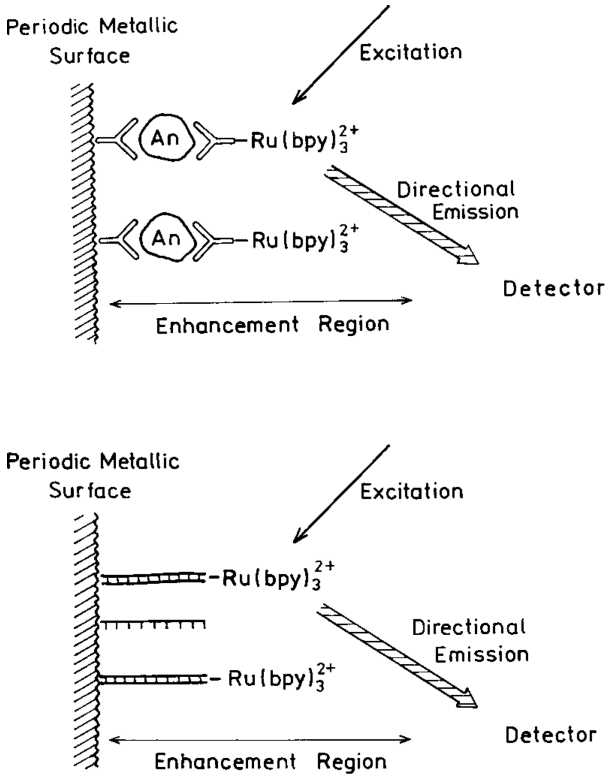

FIG. 31.

Use of metal islands on a periodic metallic surface in immunoassays, DNA hybridization assays or electroluminescent assay. The latter assays do not require an optical excitation source.

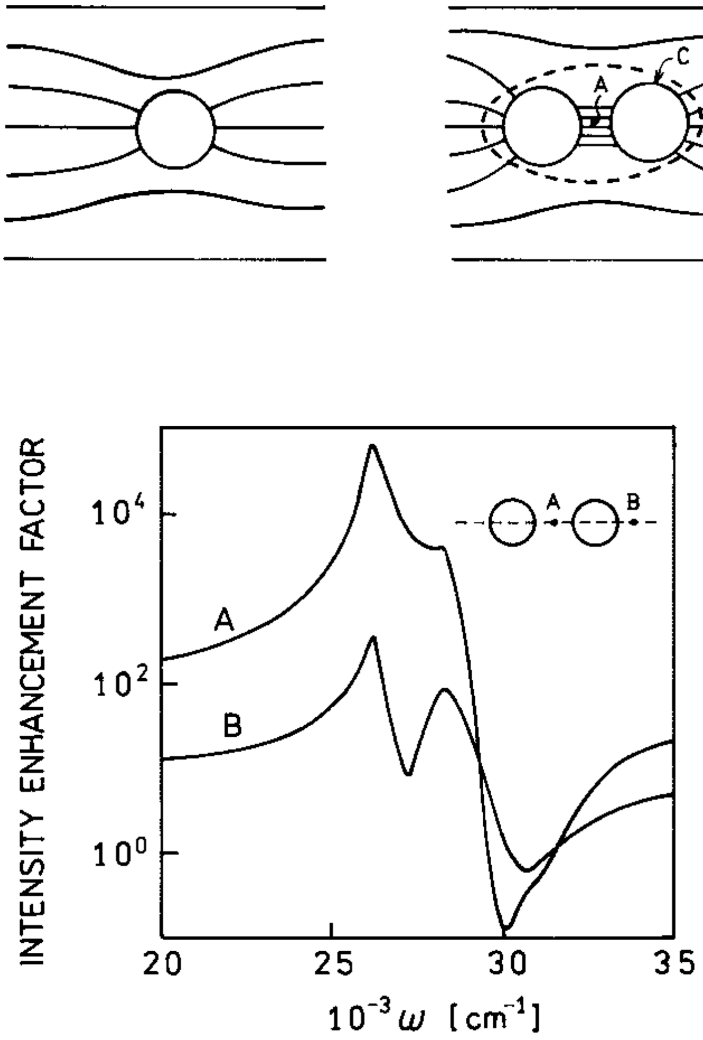

FIG. 32.

Electric field around a spheroid and between two spheroids. Points A and B have the highest fields, and point C has the lowest field. The lower panel shows the local intensities at points A and B.

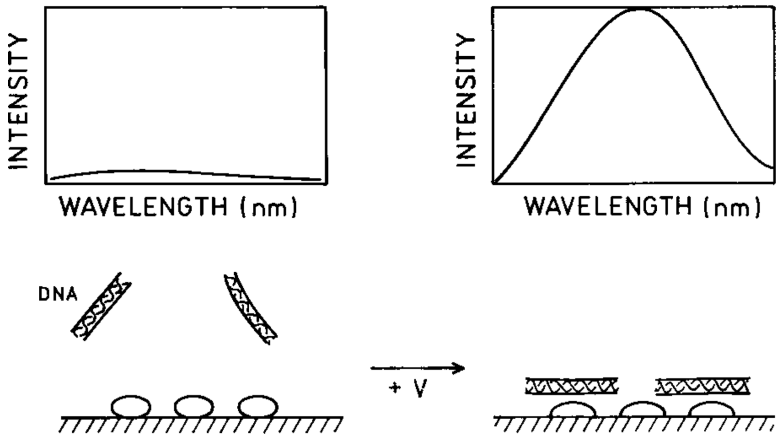

FIG. 33.
DNA analysis based on intrinsic DNA fluorescence.

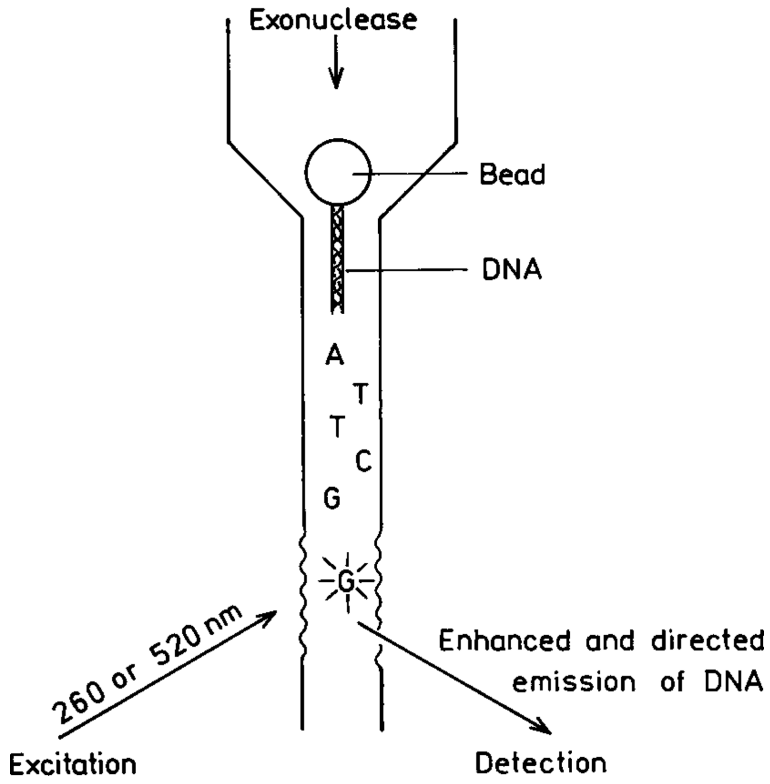

FIG. 34.
Single-strand DNA sequencing based on enhanced and directed nucleotide emission.